Look Around! Unexpected gains from training on environments in the vicinity of the target

Serena Bono[1] **Spandan Madan**[2,3] **Ishaan Grover**[1] **Mao Yasueda**[3,4]
Cynthia Breazeal[1] **Hanspeter Pfister**[2] **Gabriel Kreiman**[3*]

[1]MIT Media Lab [2]Harvard SEAS [3]Boston Children's Hospital [4]Mount Holyoke College
[*]Corresponding author: gabriel.kreiman@tch.harvard.edu

Abstract

Solutions to Markov Decision Processes (MDP) are often very sensitive to state transition probabilities. As the estimation of these probabilities is often inaccurate in practice, it is important to understand when and how Reinforcement Learning (RL) agents generalize when transition probabilities change. Here we present a new methodology to evaluate such generalization of RL agents under small shifts in the transition probabilities. Specifically, we evaluate agents in new environments (MDPs) in the vicinity of the training MDP created by adding quantifiable, parametric noise into the transition function of the training MDP. We refer to this process as *Noise Injection*, and the resulting environments as δ-*environments*. This process allows us to create controlled variations of the same environment with the level of the noise serving as a metric of distance between environments. Conventional wisdom suggests that training and testing on the same MDP should yield the best results. However, we report several cases of the opposite—when targeting a specific environment, training the agent in an alternative noise setting can yield superior outcomes. We showcase this phenomenon across 60 different variations of ATARI games, including PacMan, Pong, and Breakout.

1 Introduction

Markov Decision Processes (MDPs) are a well-established formulation to model and solve sequential decision-making problems [Bertsekas, 2012; Puterman, 2014]. A MDP is typically described by a State Space $\mathcal{S}$, an Action Space $\mathcal{A}$, a Transition Function $\mathcal{T}$ that specifies the transition probabilities between states given an action, and a Reward Function $\mathcal{R}$ denoting reward for every state-action pair [Cederborg *et al.*, 2015]. In practice, these parameters and transition probabilities are assumed known or estimable with reasonable precision [Bäuerle and Glauner, 2022; Goyal and Grand-Clement, 2023]. However, several works have showcased the difficulty in accurately estimating transition probabilities [Abbad *et al.*, 1990; Kalyanasundaram *et al.*, 2002; Feinberg and Shwartz, 2012], and their large impact on the

solution which often deteriorates as transition probabilities are changed [Xu and Mannor, 2010; Nilim and El Ghaoui, 2005; Suilen *et al.*, 2022; Moos *et al.*, 2022a].

In stark contrast to these works, here we report several cases of the opposite phenomenon—we show that a shift in the transition probabilities between the training and testing environments can actually help under certain conditions. This observation is in contrast to conventional wisdom which suggests that the best approach to perform well on a target MDP is to train an RL agent on the same target MDP.

We explored zero-shot policy transfer where a policy trained in one environment is tested on a different environment. We extend past works which focus on uncertainty in the transition probabilities [Nilim and El Ghaoui, 2005; Moos *et al.*, 2022a; Goyal and Grand-Clement, 2023], and propose a novel framework for studying policy transfer in environments with controlled, quantifiable distribution shifts in the transition probabilities.

Our framework introduces these shifts by pre-computing the transition function of an MDP, and adding small Gaussian noise to its entries, as shown in Fig. 1(a). For brevity, we refer to this approach as *Noise Injection* and the resulting new MDPs as δ-*environments*. Starting with an environment ($\mathcal{M}_T$), noise is sampled and added to it to obtain the new MDP ($\mathcal{M}_\delta$). Noise addition introduces several non-standard transitions, which had 0 probability in the original MDP as shown in Fig. 1(a). Multiple such environments can be created by sampling noise, and the distance between these worlds can be quantified by the added noise. This approach allows us to create multiple worlds in the vicinity of a target MDP, with quantitative control over the variations in the transition probabilities. An increase in the standard deviation of the Gaussian noise results in increasingly perturbed MDPs. We report experiments with Noise Injection on multiple domains across three ATARI games—PacMan, Pong, and Breakout as shown in Fig. 1 (b), (c), and (d), respectively.

To study policy transfer we define two agents as shown in Fig. 1(e). Firstly, a *Learnability Agent* which is trained and tested on the same target MDP ($\mathcal{M}_\delta$), and a *Generalization Agent* which is trained on a different environment($\mathcal{M}_T$) but tested on the target MDP ($\mathcal{M}_\delta$). Conventional wisdom suggests that agents trained on $\mathcal{M}_\delta$ will outperform agents trained on $\mathcal{M}_T$ when evaluated on $\mathcal{M}_\delta$. However, our study across 60 MDPs built on ATARI games reveals a surpris-
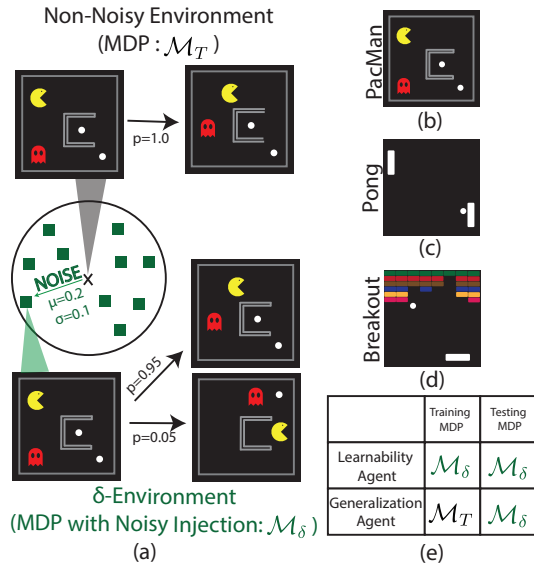
Figure 1: *ATARI games modified with Noise Injection.* (a) In the original Target Environment($\mathcal{M}_T$), when the agent (PacMan) moves right, PacMan moves right with probability 1.0. Noise Injection allows us to create multiple worlds in the vicinity of this environment by adding controlled Gaussian noise (δ) to the original Transition Function (T). When the agent takes the action *right* in these $\delta-$environments, with a low probability the game may transition to a state which would not be possible in non-noisy PacMan. For brevity, we refer to these transitions as non-standard transitions which are 0 probability in the original Target, but are now possible. Experiments with noise injection are presented on three ATARI games—(b) Pac-Man, (c) Pong, and (d) Breakout. (e) We compare two agents with these environments—a Learnability agent trained and tested on the same target environment ($\mathcal{M}_\delta$), and a Generalization agent trained on a different MDP ($\mathcal{M}_T$) and tested on $\mathcal{M}_\delta$.

ing finding—there are several cases where the Generalization Agent ($\mathcal{G}_T$) outperformed the Learnability Agent ($\mathcal{L}_\delta$).

We validated that this finding extends beyond our setup of noise injection and δ-environments, and also holds true for target MDPs differing in terms of the stochasticity of game elements. This includes variations in the distribution of the Ghost for PacMan, and the computer bar in the Pong. For brevity, we refer to these as semantic variations in MDPs. More details on their construction are provided in Sec. 4.4. We observed the same phenomenon in semantic variations as well—at times, training an agent on a different MDP resulted in better performance than training on the target MDP itself.

Finally, to better understand this phenomenon we analyzed the exploration patterns of the Learnability ($\mathcal{L}_\delta$) and Generalization Agent ($\mathcal{G}_T$) agents, and the corresponding policies learned by them. Our analyses revealed that $\mathcal{L}_\delta$ agents outperformed $\mathcal{G}_T$ agents only in scenarios where they were able to explore a unique, significantly larger set of State-Action pairs as compared to the $\mathcal{G}_T$ agents. In contrast, when when there were no differences in their exploration, the performance of the $\mathcal{G}_T$ aligned or exceeded that of the $\mathcal{L}_\delta$ agent.

2 Preliminaries: Reinforcement Learning

Similar to [Cederborg *et al.*, 2015], our work considers Reinforcement Learning (RL) as a group of algorithms designed to solve problems formulated as Markov Decision Processes (MDPs). A Markov Decision Process is characterized by the tuple $(\mathcal{S}, \mathcal{A}, \mathcal{T}, \mathcal{R}, \lambda)$, representing the collection of potential world states ($\mathcal{S}$), space of actions ($\mathcal{A}$), the transition function ($\mathcal{T} : \mathcal{S} \times \mathcal{A} \to \mathcal{P}(\mathcal{S})$), the reward function ($\mathcal{R} : \mathcal{S} \times \mathcal{A} \to \mathcal{R}$), and a discount factor ($0 < \lambda \leq 1$). The objective is to identify policies ($\pi : \mathcal{S} \times \mathcal{A} \to \mathcal{R}$) that maximize cumulative rewards.

Q-learning [Watkins and Dayan, 1992] and SARSA [Rummery and Niranjan, 1994] are two algorithms to learn such policies. Both Q-Learning and SARSA algorithms update the Q-values of state-action pairs, but they differ in their approaches. Q-Learning focuses on the maximum expected future rewards, and updates Q-values using the formula:

$$Q(s,a) \leftarrow Q(s,a) + \alpha \left[r + \gamma \max_{a'} Q(s',a') - Q(s,a) \right] \tag{1}$$

where α is the learning rate, γ is the discount factor, and s, s', a, a', r represent the current state, next state, current action, next action, and immediate reward, respectively.

On the other hand, SARSA updates Q-values based on the actual policy's actions with the formula:

$$Q(s,a) \leftarrow Q(s,a) + \alpha \left[r + \gamma Q(s',a') - Q(s,a) \right] \tag{2}$$

Here the update incorporates both immediate rewards and the Q-value of the actual next action taken.

Agents need to balance two critical aspects: exploration and exploitation. Exploration involves trying potentially less optimal actions to understand the environment better. Conversely, exploitation means choosing actions known to yield high rewards. We report results with the Boltzmann and the ϵ-greedy exploration strategies. Boltzmann exploration determines the probability of selecting an action as follows:

$$Pr_q(a) = \frac{e^{Q(s,a)/\tau}}{\sum_{a'} e^{Q(s,a')/\tau}} \tag{3}$$

The constant τ is referred to as the temperature. On the other hand, the ϵ-greedy strategy is simpler and more direct—the agent selects a random action with probability ϵ, and the action with the highest Q-value with probability $1 - \epsilon$.

3 Related Works

3.1 Generalization in Reinforcement Learning

Generalization in Reinforcement Learning (RL) aims to learn policies that perform well in novel, unseen environments at the time of deployment [Kirk *et al.*, 2021; Moos *et al.*, 2022b; OpenAI *et al.*, 2019; Filos *et al.*, 2020; Biedenkapp *et al.*, 2020]. Recent years have seen several generalization benchmarks, which includes variations in the state space [Hafner, 2021], dynamics [Dulac-Arnold *et al.*, 2019], observation [Zhu *et al.*, 2020], reward function [Bapst *et al.*, 2019], and new game levels [Justesen *et al.*, 2018], among others. Broadly, these works can be divided into two categories.
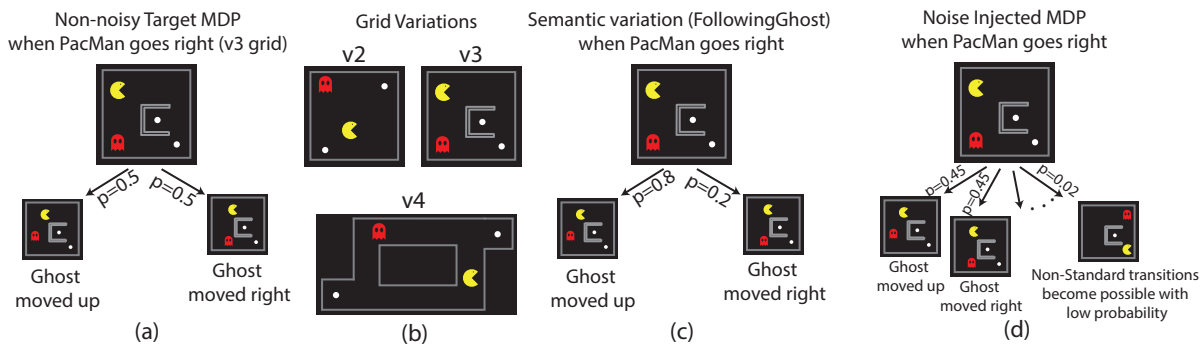
Figure 2: *Variations for PacMan.*(a) Game dynamics when the agent picks the action *right* in a standard, non-noisy MDP for the v3 Grid. Ghosts follow a uniform distribution over possible moves and move *up* or *right* with an equal probability of 0.5. This is referred to as a RandomGhost. (b) Grid variations for PacMan—v2, v3, and v4. These grids vary in grid size, positions of walls, and positions of food pellets. v2, v3, and v4 are designed to be increasingly hard. (c) Semantic variations involves changing the distribution of stochastic game elements. Here, a FollowingGhost is depicted which has a higher probability of taking a move which brings it closer to the PacMan (0.8). (d) Noise injected MDP generated by adding gaussian noise to the standard Transition Function. Alongside states reachable by the ghost taking a legal move, non-standard transitions now become possible which result in the game reaching states otherwise unreachable—ghost and PacMan arrive to the right hand corners of the grid in a single step with a non-zero probability.

Firstly, Procedural Content Generation which involves creation of diverse and dynamic environments based on algorithms driven by a seed value. Examples of this include OpenAI Procgen benchmark [Cobbe *et al.*, 2020] and the Distracting Control Suite [Stone *et al.*, 2021]. Secondly, recent work on Controllable Environments [Kirk *et al.*, 2021] allows explicit manipulation of individual components as parameters of the environment, providing more granular control. CausalWorld [Ahmed *et al.*, 2020], RWRL [Dulac-Arnold *et al.*, 2019], Alchemy [Wang *et al.*, 2021], Meta-world [Yu *et al.*, 2019] are examples of such parametric worlds. A major drawback in these benchmarks is the difficulty in concretely quantifying the distribution shifts between the train and test MDPs. In contrast, our methodology allows for a concrete and parametric definition for this distribution shift, and allows explicit modification of transition probabilities.

3.2 Inspiration from controlled analysis of generalization behaviour in visual recognition

We draw inspiration from work studying generalization under controlled, quantifiable distribution shifts. This includes shifts in 3D rotations [Mondal *et al.*, 2022; Madan *et al.*, 2023], category-viewpoint combinations [Madan *et al.*, 2022a], incongruent scene context [Bomatter *et al.*, 2021], novel light and viewpoint combinations [Sakai *et al.*, 2022], object materials [Madan *et al.*, 2022b], and non-canonical viewpoints [Barbu *et al.*, 2019], among others. Inspired by these, we characterize generalization in RL through carefully constructed environments with a consistent metric defining the distribution shifts between environments.

4 Generating MDPs for investigating generalization

We created 60 different MDPs across three ATARI games (PacMan, Pong, and Breakout) by varying grid layouts, distributions defining the stochasticity of different game elements,

and modifying transition probabilities using Noise Injection (See Fig. 2 and Table. 1). Here we outline these variations.

4.1 Domains

We implemented all three ATARI games from scratch, building on the Berkeley PacMan Projects [DeNero *et al.*, 2014]. PacMan was modelled as an MDP characterized by the tuple $(\mathcal{S}, \mathcal{A}, \mathcal{T}, \mathcal{R}, \lambda)$. Below we define these:

State (s) and State Space ($\mathcal{S}$): We represented a grid of size $M \times N$ as a matrix of the same shape with the entries corresponding to the game element occupying the position in the grid—p (PacMan), g (Ghost), f (Food), w (Wall), or e (Empty). States were computed by unrolling this matrix into a vector of length $M * N$. The state space $\mathcal{S}$ refers to the set of all possible states.

Action Space ($\mathcal{A}(s)$): Set of legal actions PacMan could take in state s. PacMan can move Left, Right, Up, or Down but not enter walls. Thus, when the PacMan is at the top left position the set of legal actions was only Right, Down.

Transition Matrix ($\mathcal{T}(s_i, a, s_j)$): Probability of moving to state s_j if the agent took action a at state s_i (see Fig. 2(a)).

Reward Function ($\mathcal{R}(s)$): PacMan received +20 for eating a food pellet, -1 for every time step, -200 when it was killed, and +500 for finishing the game. [Cederborg *et al.*, 2015].

Game Stochasticity: The motion of PacMan is deterministic—a Left action (if legal) will ensure that PacMan moves left. However, ghosts move stochastically according to a pre-fixed distribution. For instance, a RandomGhost moves in all directions with equal probability (accounting for walls). Thus, the game is non-deterministic.

MDPs for Pong and Breakout are defined analogously. For additional details, please refer to Supplementary Sec. A.

4.2 Grid Variations of ATARI games

We build on past work [Biedenkapp *et al.*, 2020], and train RL agents on the *v2*, *v3*, *v4* grids for PacMan as depicted in Fig. 2(b). For Pong and Breakout we report results on two

ATARI Game	Grid Variations	Noise Injected Variations	Semantic Variation	Total
PacMan	v2, v3, v4	$\delta = 0$ (No Noise) $\delta \sim \mathcal{N}(0, 0.1)$ $\delta \sim \mathcal{N}(0, 0.5)$	RandomGhost FollowingGhost ($p = 0.3, 0.6$) TeleportingGhost ($p = 0.5, 0.2$)	33
Pong	p1, p2	$\delta = 0$ (No Noise) $\delta \sim \mathcal{N}(0, 0.1)$ $\delta \sim \mathcal{N}(0, 0.5)$	RandomPaddle FollowingPaddle ($p = 0.3, 0.6$)	18
Breakout	b1, b2, b3	$\delta = 0$ (No Noise) $\delta \sim \mathcal{N}(0, 0.1)$ $\delta \sim \mathcal{N}(0, 0.5)$	-	9

Table 1: **Oveview of experimental protocol.** Our experiments include multiple variations of three ATARI games—PacMan, Pong, and Breakout. For each game, we have multiple grid variations of increasing difficulty. When introducing variations in these grids with noise injection, we report results for two levels of added noise—a low-noise setting: $\delta \sim \mathcal{N}(0, 0.1)$, and a high-noise setting: $\delta \sim \mathcal{N}(0, 0.5)$. Furthermore, for each grid we introduce further variations by modifying the distribution of the stochastic game element (ghost in PacMan, and the computer paddle in Pong). In all, we report results on 60 MDPs across these games.

(*p1* and *p2*) and three grids (*b1*, *b2*, and *b3*) respectively (see Supplementary Fig. Sup1 and Fig. Sup2). These grids are designed to be increasingly hard for RL agents, and confirm that our findings are not an artefact of a specific ATARI game or grid.

4.3 Noise Injection: Generating new, controlled environments in the vicinity of an MDP

We generate controlled variations of a target MDP by explicitly computing its Transition Function and then adding sampled noise to it. Below we outline this process:

Explicit enumeration of all states: We first enumerate all possible states by representing the game as a tree, and recursively rolling out all possible actions and moves by the agent and stochastic game elements. For PacMan, these correspond to the PacMan and the ghosts. For Pong, these correspond to the two paddles. For Breakout, the single paddle.

Explicit computation of Transition Function: With all states enumerated, $\mathcal{T}(s_i, a, s_j)$ can be computed explicitly. As the movement of all elements is independent, $\mathcal{T}(s_i, a, s_j)$ was computed by multiplying the probability of each element moving from its grid-position in s_i to its grid-position in s_j.

Creating $\delta-$environments: The new transition function for a δ-enrivonment is denoted $\mathcal{T}_\delta = \mathcal{T} + \delta$, with $\delta \sim \mathcal{N}(\mu, \sigma)$ sampled i.i.d. before every game to ensure randomization. Then, $\mathcal{T}_\delta$ is normalized to ensure all probabilities $p_{i,j}$ for all possible transitions from a given state s_i and action a to any successor state s_j sum to 1:

$$\mathcal{T}_\delta(s_j, a, s_i) = \frac{|\mathcal{S}|p_{i,j} + \delta_{i,j}}{|\mathcal{S}| + \sum_j \delta_{i,j}} \quad (4)$$

$|\mathcal{S}|$ denotes the number of states, and guarantees the probability of legal successors does not approach 0 as the state space grows. We investigated two settings—(i) *Low-Noise* with $\delta \sim \mathcal{N}(0, 0.1)$, where some non-standard transitions previously impossible without noise are now possible with a low probability. (ii) *High-Noise* with $\delta \sim \mathcal{N}(0, 0.5)$, where non-standard transitions are possible with higher probability.

4.4 Semantic variations of ATARI games

PacMan Variations: We modified PacMan by changing the distribution of the ghost in three different ways:

- *RandomGhost*: Let l_s denote possible legal moves for the ghost given state s. A RandomGhost samples move $m \sim Unif(l_s)$. Thus, ghost movement is randomly sampled from legal moves with equal probability.

- *FollowingGhost (p)*: Ghost follows PacMan with probability p—picks the legal move which minimizes the Manhattan Distance between the ghost and PacMan. The ghost picks one of the remaining legal moves with probability $(1 - p)/(|l_s| - 1)$, where $|l_s|$ denotes total legal moves. We report results for $p = 0.3, 0.6$.

- *TeleportingGhost (p)*: The ghost picks one of Left, Right, Up, Down with probability $p/4$ each. If the chosen action is not permissible (i.e., it runs into a wall), the ghost teleports to a random position on the grid. With probability $1-p$, the ghost behaves like a RandomGhost.

Pong Variations: We focus on the single-player Pong— the RL agent controlled one paddle and aimed to outperform a computer-controlled paddle. Variations were introduced by altering the distribution of the computer-controlled paddle:

- *RandomPaddle*: Next move $m \sim Unif(l_s)$, where l_s denotes set of legal moves.

- *FollowingPaddle (p)*: Computer-controlled paddle follows the ball with probability p (minimizing manhattan distance), and functions as RandomPaddle with probability $1 - p$. Setting $p = 1$ guarantees the computer never loses. We report results for $p = 0.3, 0.6$.

5 Experimental Details

5.1 Evaluation metric

We compared the mean reward curve of Learnability and Generalization agents. An agent $\mathcal{G}_T$ is said to generalize well with respect to $\mathcal{M}_\delta$, if its mean reward is as good as the corresponding learnability agent $\mathcal{L}_\delta$.
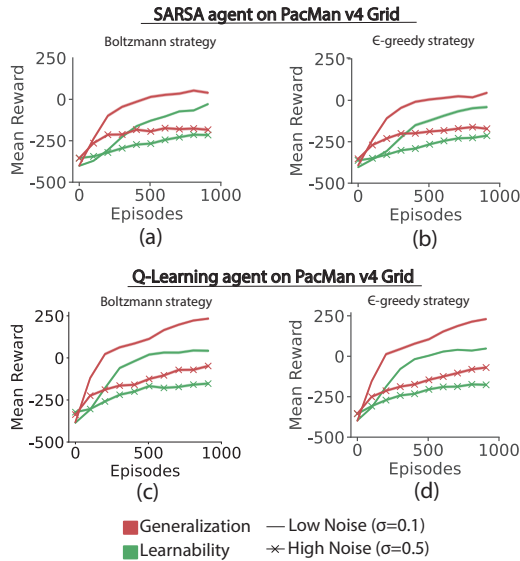
Figure 3: *Generalization agents can outperform Learnability agents.* Results for PacMan v4 grid reporting mean reward as a function of episode number. (a) SARSA agent trained with a Boltzmann exploration strategy. For Target MDPs generated with both high (solid line) and low (line with 'x' markers) level noise injection, the Generalization Agent (red) beats the Learnability Agent (green). (b) The same result holds for a SARSA agent trained with the ϵ−greedy exploration strategy. This finding also holds for Q-Learning agents trained with (c) Boltzmann and (d) ϵ−greedy exploration strategies. Noise added to the transition function is sampled $\delta \sim \mathcal{N}(0, 0.1)$ in Low-Noise and $\delta \sim \mathcal{N}(0, 0.5)$ in High-Noise settings.

5.2 Learning algorithm and Evaluation details

Agents are trained with both tabular Q-Learning [Watkins and Dayan, 1992] and SARSA Q-learning [Rummery and Niranjan, 1994], using Boltzmann or ϵ-greedy exploration strategies. In particular, we trained agents for 1000 episodes and averaged results over 500 trained agents. After every 10 training episodes, agents were evaluated using 10 testing episodes. We report the mean reward curves at convergence. Hyperparameters were inherited from past work [Cederborg *et al.*, 2015] and are available in the supplement in Sec. B.

6 Results

We report findings from the Generalization and Learnability agents trained with the multiple variations of PacMan, Pong, and Breakout as described in Sec. 4 and Table 1.

6.1 There exist several MDPs where Generalization Agents outperform the Learnability Agents.

The mean reward increases with training, as expected (Fig. 3). Also, as intuitively expected, agents achieved higher performance under conditions of low noise compared to high noise (Fig. 3, compare solid lines versus lines with 'x' markers). Less intuitive was the relationship between Generalization and Learnability agents. Fig. 3, shows mean reward curves for multiple RL agents trained to solve the PacMan v4
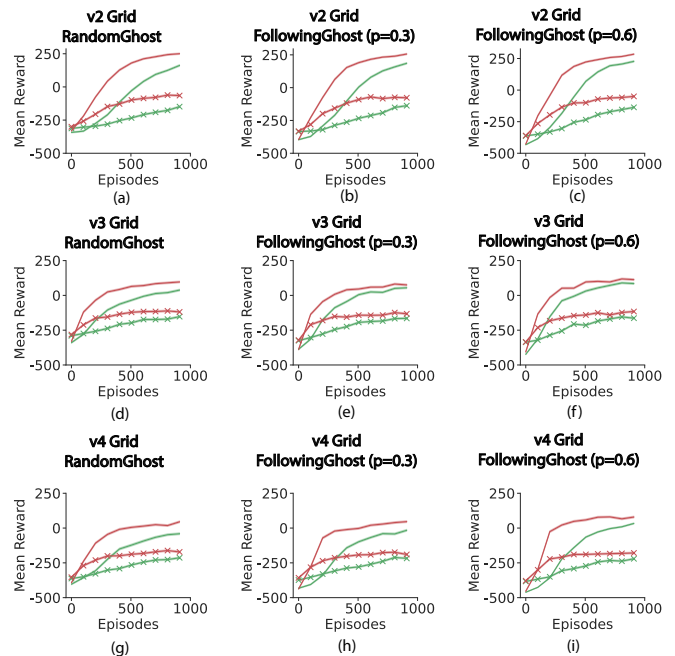
Figure 4: *Generalization can outperform Learnability across multiple variations of PacMan.* (a) Agents trained on the PacMan v2 grid with the Ghost dynamics set to the RandomGhost setting—the ghost picks a move from all possible legal moves with an equal probability. (b) Agents trained on v2 with a DirectionalGhost with $p = 0.3$—ghost has probability of 0.3 to move in a pre-specified direction (here *right*), and a probability of 0.7 of picking one of the remaining moves (each remaining move equally likely). (c) DirectionalGhost with $p = 0.6$. (d),(e),(f) Variations with the v3 grid with RandomGhost, DirectionGhost ($p = 0.3$) and DirectionalGhost ($p = 0.6$) respectively. (g),(h),(i) Same variations with the v4 grid. All experiments are shown for SARSA agents trained with the ϵ−greedy exploration strategy. Generalization agents consistently beat Learnability Agents across multiple Target MDPs which vary in the grid complexity and game stochasticity (ghost behaviour).

Grid with RandomGhosts, including Q-Learning and SARSA agents trained with the Boltzmann and ϵ−greedy exploration strategies. The Learnability agent was trained on the noise injected target MDP, while the generalization agent is trained on the non-noisy MDP, and then both agents evaluated on the Target noise-injected environment. Intriguingly, the Generalization agents (Fig. 3, red) consistently outperformed the Learnability agents (Fig. 3, green). This gap continued until convergence at 1000 episodes, was observed across both low and high noise levels, and was apparent for SARSA and Q-Learning, for Boltzman and ϵ−greedy exploration strategies.

To assess whether this observation was dependent on the target MDP, we replicated these findings on multiple PacMan grids and stochastic variations. These results are presented in Fig. 4 for 9 different target MDPs for Generalization and Learnability agents trained with SARSA and the ϵ−greedy strategy. In several cases, the Generalization agents beat the Learnability agents, for both low and high levels of noise. Corresponding results for agents trained with SARSA + Boltzmann exploration strategy, and for Q-Learning with
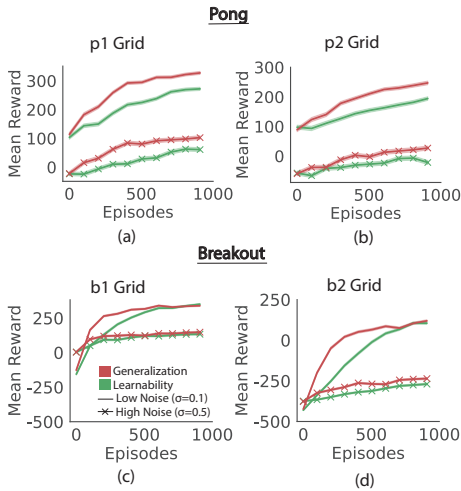
Figure 5: *Mean Reward Curves for Learnability and Generalization Agents for Pong and Breakout.* Performance of SARSA agents trained with a $\epsilon-$greedy exploration strategy on (a) Pong p1 grid, (b) Pong p2 grid, (c) Breakout b1 grid, and (d) Breakout b2 grid. The Generalization Agent beats the Learnability Agent for Target MDPs created with both high and low noise for all grids.

Figure 6: *Rewards across semantic variations of PacMan and Pong.* (a) Given the target PacMan MDP with the v2 grid and TeleportingGhost, the Generalization trained on the RandomGhost outperformed the Learnability agent that was trained and tested on the same Target MDP (TeleportingGhost). (b) This finding extends to TeleportingGhost and RandomGhost MDPs with the PacMan v3 Grid as well. (c) For the Pong p1 grid, Generalization agents trained on an MDP with DirectionalPaddle performed better on the RandomPaddle MDP during testing, as compared to the Learnability Agent trained and tested on the RandomPaddle MDP. (d) The same finding extends to the p2 grid as well.

both $\epsilon-$greedy and Boltzmann exploration strategies are in Supplementary Figures Sup3, Sup4 and Sup5.

We also extended these findings to two additional ATARI games to evaluate if these extend to other games. Fig. 5 reports these findings for Pong and Breakout. We report results for multiple grids for each, for agents trained with SARSA and $\epsilon-$greedy strategy. These experiments confirmed that Generalization agents can outperform Learnability agents consistently across several ATARI environments. Corresponding agents trained with Q-Learning and different exploration strategies are reported in the Supplementary Figs. Sup6, Sup7, Sup8, Sup9, Sup10, Sup11, and Sup12. In these plots we compare generalization and learnability agents of 18 variations for Pong and 9 variations for Breakout.

In sum, there exist several MDPs where it is better to train on a different MDP than the target MDP. To the best of our knowledge, these results provide the first evidence suggesting that training on a different MDP can enable more efficient policy learning than training on the target environment. In doing so, our finding fundamentally challenges our understanding of the generalization capabilities of RL agents under shifts in transition probabilities.

6.2 Generalization agents also thrive in semantically meaningful δ-environments

Results presented so far focused on MDPs generated by noise injection. We further confirmed that analogous trends also hold true for semantic variations of the two ATARI Games (see Sec. 4.4). We denote these alternate semantic environments as $\mathcal{M}_{T'}$ (semantic noise), as opposed to $\mathcal{M}_\delta$ in the case of noise injection.

For PacMan, Learnability agents were trained and tested using TeleportingGhosts ($\mathcal{M}_{T'}$), while the Generalization agents were trained with PacMan with RandomGhosts ($\mathcal{M}_T$)

and then tested on TeleportingGhosts ($\mathcal{M}_{T'}$) (Fig. 6a, b). Even under these semantic noise conditions, Generalization agents outperformed Learnability agents. These results provide compelling evidence suggesting these findings extend beyond the vicinity of MDPs.

In the case of Pong, we report analogous results with $\mathcal{M}_{T'}$ set to FollowingPaddle, and $\mathcal{M}_T$ set to RandomPaddle. As shown in Fig. 6(c) and (d), Generalization agents also outperformed Learnability agents (by a smaller margin) in both the p1 and p2 grids. These results are for SARSA agents trained with $\epsilon-$greedy exploration strategy. Analogous results for Pong with Q-Learning and other exploration strategies are reported in Supplementary Figs. Sup16, Sup17, Sup18, Sup19, Sup20, Sup21, Sup22, Sup23

6.3 The exploration patterns of state-action pairs can predict differences between Generalization and Learning agents

So far, we have presented comprehensive analyses with several examples of our main finding—Generalization Agents beating Learnability Agents. Here, we present a potential explanation for this counter-intuitive phenomenon.

Noise Injection modifies MDPs such that non-standard transitions become increasingly probable as noise is added. Intuitively, $\mathcal{L}_\delta$ trained on the noisy environment should be able to explore significantly more states and acquire knowledge about these low-probability transitions. This would enable it to beat $\mathcal{G}_T$, as conventional wisdom suggests. This motivated us to compare the exploration patterns for $\mathcal{L}_\delta$ and $\mathcal{G}_T$ to explain the gap in their performance.
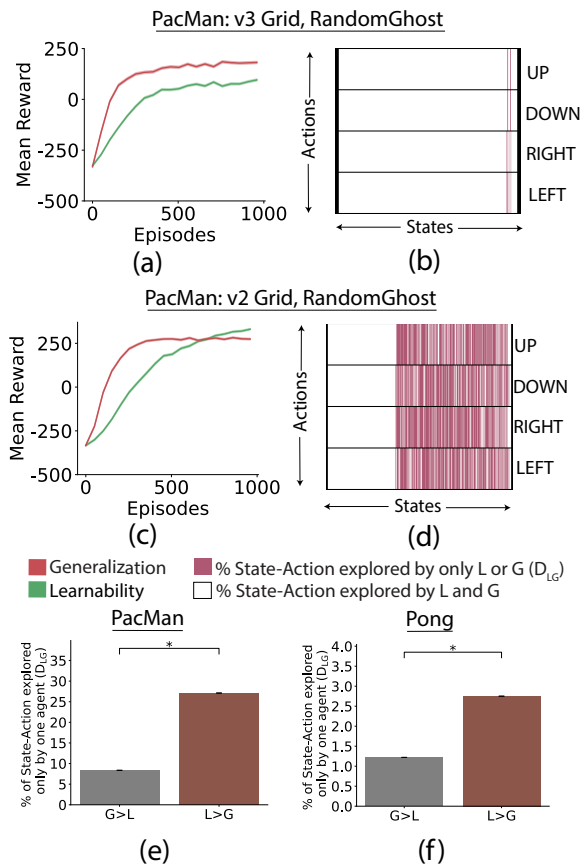
Figure 7: *Exploration patterns predict the reward gap between* $\mathcal{L}_\delta$ *and* $\mathcal{G}_T$. (a) Reward for agents trained on PacMan v3, where $\mathcal{G}_T$ outperforms $\mathcal{L}_\delta$. (b) The *exploration grid* visualizing the difference in State-Action (S-A) pairs explored by these agents (D_{LG}). Each cell corresponds to one S-A Pair, and the color denotes which agents visited this S-A pair. In this case, a negligible fraction of S-A pairs were visited only by one agent (pink). (c) Rewards for agents trained on PacMan v3. Here, $\mathcal{G}_T$ performs worse than $\mathcal{L}_\delta$. (d) Corresponding exploration shows a large fraction of pairs were only visited by the $\mathcal{L}_\delta$ agent. (e) D_{LG} averaged over PacMan grids where $\mathcal{G}_T$ outperformed $\mathcal{L}_\delta$ and vice-versa. (f) D_{LG} averaged over Pong grids.

We enumerate all State-Action Pairs, and divide them into three groups—(i) Fraction of state-action (S-A) pairs explored by both agents (P_{LG}), (ii) pairs explored only by the Learnability Agent (P_L), and (iii) pairs explored only by the Generalization agent (P_G). Thus, $P_{LG} + P_L + P_G = 1$. We denote the feature $D_{LG} = P_L + P_G$, which measures the divergence in the exploration patterns of these two agents.

In Fig. 7 we visualize D_{LG} for grids where $\mathcal{G}_T$ outperformed $\mathcal{L}_\delta$ agents, and where it did not. Fig. 7(a) shows an agent trained with Q-Learning and Boltzmann exploration strategy for the PacMan v3 grid with RandomGhost stochasticity. Here, $\mathcal{G}_T$ beats the $\mathcal{L}_\delta$ agent. The corresponding panel Fig. 7(b) depicts D_{LG} visually—each cell of this grid represents an S-A pair, and its color denotes which of the two agents explored the particular S-A pair. We refer to this as the *exploration grid* for these agents. Here, the exploration

grid shows that most S-A pairs were explored by both agents, with no significant differences in their exploration patterns. In contrast, Fig. 7(c, d) report these numbers for PacMan v2 which are starkly different. Here, the $\mathcal{G}_T$ agent performs worse than the $\mathcal{L}_\delta$ agent, and the exploration grid reveals there is a very high fraction of S-A pairs explored only by the $\mathcal{L}_\delta$ agent. These figures visually depict the relationship between D_{LG} and the Reward Gap between the two agents which we denote as $R_{LG} = R_L - R_G$.

Fig. 7(e) reports the mean value of D_{LG} across all PacMan MDPs created with noise injection. On average, D_{LG} is significantly higher in MDPs where $\mathcal{L}_\delta$ outperformed $\mathcal{G}_T$, than when it did not (two-sided t-test, $p < 0.05$). The same result holds true for Pong MDPs as reported in Fig. 7(f). Exploration grids and additional results for variations of PacMan, Pong, and Breakout can be found in the supplement in Sec. **??**.

Next, we conducted a correlation analysis to better understand the impact of exploration patterns on the reward gap between these two agents. The Spearman correlation coefficient between D_{LG} and R_{LG} was found to be $0.43 (p < 0.005)$ for PacMan and $0.26 (p < 0.005)$ for Pong indicating a moderate positive monotonic relationship between the two variables. Combined, these analyses show that the Reward Gap between these agents is driven by the differences in their exploration patterns under noisy transition probabilities. $\mathcal{L}_\delta$ agents can beat $\mathcal{G}_T$ agents, but only when they successfully explore a large, unique set of State-Action pairs which the $\mathcal{G}_T$ agent is not able to. In the absence of a substantial difference in their exploration patterns, Generalization agents perform better, or as well as, Learnability agents.

7 Discussion

Here, we propose a new methodology to evaluate robustness of RL agents by generating new MDPs in the vicinity of the target with a metric to quantify the distance between these environments. This approach led us to discover a striking phenomenon—sometimes, training an agent on alternative MDPs can lead to outcomes even better than training on the target MDP itself. This phenomenon occurred across multiple algorithms and exploration strategies (Fig. 3), grid layouts and game stochasticity (Fig. 4), and multiple ATARI games (Fig. 5). We also showed that this phenomenon extends beyond Noise Injected environments, and can also occur when semantic changes are introduced in game elements(Fig. 6). Finally, we showed that this reward gap between the two agents appears to be driven by the exploration patterns of the agents under different transition probabilities (Fig. 7).

This phenomenon fundamentally challenges conventional wisdom regarding generalization under shifts in transition probabilities. Real-world applications often require modeling the environment stochasticity, and understanding the susceptibilities of RL agents under small errors in estimating or modeling this stochasticity is imperative to build robust agents that can be deployed with confidence. Thus, we strongly believe that the tools and analyses presented in this work can benefit the RL, Planning, and Robotics communities by shedding light on the generalization behaviour of RL

agents under subtle shifts in transition probabilities.

References

[Abbad *et al.*, 1990] Mohammed Abbad, Jerzy A Filar, and Tomasz R Bielecki. Algorithms for singularly perturbed limiting average markov control problems. In *29th IEEE Conference on Decision and Control*, pages 1402–1407. IEEE, 1990.

[Ahmed *et al.*, 2020] Ossama Ahmed, Frederik Träuble, Anirudh Goyal, Alexander Neitz, Manuel Wüthrich, Yoshua Bengio, Bernhard Schölkopf, and Stefan Bauer. Causalworld: A robotic manipulation benchmark for causal structure and transfer learning. *CoRR*, abs/2010.04296, 2020.

[Bapst *et al.*, 2019] Victor Bapst, Alvaro Sanchez-Gonzalez, Carl Doersch, Kimberly L. Stachenfeld, Pushmeet Kohli, Peter W. Battaglia, and Jessica B. Hamrick. Structured agents for physical construction. *CoRR*, abs/1904.03177, 2019.

[Barbu *et al.*, 2019] Andrei Barbu, David Mayo, Julian Alverio, William Luo, Christopher Wang, Dan Gutfreund, Josh Tenenbaum, and Boris Katz. Objectnet: A large-scale bias-controlled dataset for pushing the limits of object recognition models. *Advances in neural information processing systems*, 32, 2019.

[Bäuerle and Glauner, 2022] Nicole Bäuerle and Alexander Glauner. Distributionally robust markov decision processes and their connection to risk measures. *Mathematics of Operations Research*, 47(3):1757–1780, 2022.

[Bertsekas, 2012] Dimitri Bertsekas. *Dynamic programming and optimal control: Volume I*, volume 4. Athena scientific, 2012.

[Biedenkapp *et al.*, 2020] A. Biedenkapp, H. F. Bozkurt, T. Eimer, F. Hutter, and M. Lindauer. Dynamic algorithm configuration: Foundation of a new meta-algorithmic framework. In *Proceedings of the Twenty-fourth European Conference on Artificial Intelligence (ECAI'20)*, June 2020.

[Bomatter *et al.*, 2021] Philipp Bomatter, Mengmi Zhang, Dimitar Karev, Spandan Madan, Claire Tseng, and Gabriel Kreiman. When pigs fly: Contextual reasoning in synthetic and natural scenes, 2021.

[Cederborg *et al.*, 2015] Thomas Cederborg, Ishaan Grover, Charles Lee Isbell, and Andrea Lockerd Thomaz. Policy shaping with human teachers. In *International Joint Conference on Artificial Intelligence*, 2015.

[Cobbe *et al.*, 2020] Karl Cobbe, Christopher Hesse, Jacob Hilton, and John Schulman. Leveraging procedural generation to benchmark reinforcement learning, 2020.

[DeNero *et al.*, 2014] John DeNero, Dan Klein, and Pieter Abbeel. Cs188: Berkeley pacman projects. http://ai.berkeley.edu/home.html (Spring 2014), 2014.

[Dulac-Arnold *et al.*, 2019] Gabriel Dulac-Arnold, Daniel J. Mankowitz, and Todd Hester. Challenges of real-world reinforcement learning. *CoRR*, abs/1904.12901, 2019.

[Feinberg and Shwartz, 2012] Eugene A Feinberg and Adam Shwartz. *Handbook of Markov decision processes: methods and applications*, volume 40. Springer Science & Business Media, 2012.

[Filos *et al.*, 2020] Angelos Filos, Panagiotis Tigas, Rowan McAllister, Nicholas Rhinehart, Sergey Levine, and Yarin Gal. Can autonomous vehicles identify, recover from, and adapt to distribution shifts? *CoRR*, abs/2006.14911, 2020.

[Goyal and Grand-Clement, 2023] Vineet Goyal and Julien Grand-Clement. Robust markov decision processes: Beyond rectangularity. *Mathematics of Operations Research*, 48(1):203–226, 2023.

[Hafner, 2021] Danijar Hafner. Benchmarking the spectrum of agent capabilities. *CoRR*, abs/2109.06780, 2021.

[Justesen *et al.*, 2018] Niels Justesen, Ruben Rodriguez Torrado, Philip Bontrager, Ahmed Khalifa, Julian Togelius, and Sebastian Risi. Illuminating generalization in deep reinforcement learning through procedural level generation. *arXiv preprint arXiv:1806.10729*, 2018.

[Kalyanasundaram *et al.*, 2002] Suresh Kalyanasundaram, Edwin KP Chong, and Ness B Shroff. Markov decision processes with uncertain transition rates: Sensitivity and robust control. In *Proceedings of the 41st IEEE Conference on Decision and Control, 2002.*, volume 4, pages 3799–3804. IEEE, 2002.

[Kirk *et al.*, 2021] Robert Kirk, Amy Zhang, Edward Grefenstette, and Tim Rocktäschel. A survey of generalisation in deep reinforcement learning. *CoRR*, abs/2111.09794, 2021.

[Madan *et al.*, 2022a] Spandan Madan, Timothy Henry, Jamell Dozier, Helen Ho, Nishchal Bhandari, Tomotake Sasaki, Frédo Durand, Hanspeter Pfister, and Xavier Boix. When and how convolutional neural networks generalize to out-of-distribution category–viewpoint combinations. *Nature Machine Intelligence*, 4(2):146–153, 2022.

[Madan *et al.*, 2022b] Spandan Madan, Li You, Mengmi Zhang, Hanspeter Pfister, and Gabriel Kreiman. What makes domain generalization hard?, 2022.

[Madan *et al.*, 2023] Spandan Madan, Tomotake Sasaki, Hanspeter Pfister, Tzu-Mao Li, and Xavier Boix. Adversarial examples within the training distribution: A widespread challenge, 2023.

[Mondal *et al.*, 2022] Shanka Subhra Mondal, Zack Dulberg, and Jonathan Cohen. Generalization to out-of-distribution transformations, 2022.

[Moos *et al.*, 2022a] Janosch Moos, Kay Hansel, Hany Abdulsamad, Svenja Stark, Debora Clever, and Jan Peters. Robust reinforcement learning: A review of foundations and recent advances. *Machine Learning and Knowledge Extraction*, 4(1):276–315, 2022.

[Moos *et al.*, 2022b] Janosch Moos, Kay Hansel, Hany Abdulsamad, Svenja Stark, Debora Clever, and Jan Peters. Robust reinforcement learning: A review of foundations and recent advances. *Machine Learning and Knowledge Extraction*, 4(1):276–315, 2022.

[Nilim and El Ghaoui, 2005] Arnab Nilim and Laurent El Ghaoui. Robust control of markov decision processes with uncertain transition matrices. *Operations Research*, 53(5):780–798, 2005.

[OpenAI *et al.*, 2019] OpenAI, Ilge Akkaya, Marcin Andrychowicz, Maciek Chociej, Mateusz Litwin, Bob McGrew, Arthur Petron, Alex Paino, Matthias Plappert, Glenn Powell, Raphael Ribas, Jonas Schneider, Nikolas Tezak, Jerry Tworek, Peter Welinder, Lilian Weng, Qiming Yuan, Wojciech Zaremba, and Lei Zhang. Solving rubik's cube with a robot hand. *CoRR*, abs/1910.07113, 2019.

[Puterman, 2014] Martin L Puterman. *Markov decision processes: discrete stochastic dynamic programming*. John Wiley & Sons, 2014.

[Rummery and Niranjan, 1994] Gavin Adrian Rummery and Mahesan Niranjan. On-line q-learning using connectionist systems. 1994.

[Sakai *et al.*, 2022] Akira Sakai, Taro Sunagawa, Spandan Madan, Kanata Suzuki, Takashi Katoh, Hiromichi Kobashi, Hanspeter Pfister, Pawan Sinha, Xavier Boix, and Tomotake Sasaki. Three approaches to facilitate invariant neurons and generalization to out-of-distribution orientations and illuminations. *Neural Networks*, 155:119–143, 2022.

[Stone *et al.*, 2021] Austin Stone, Oscar Ramirez, Kurt Konolige, and Rico Jonschkowski. The distracting control suite – a challenging benchmark for reinforcement learning from pixels, 2021.

[Suilen *et al.*, 2022] Marnix Suilen, Thiago D Simão, David Parker, and Nils Jansen. Robust anytime learning of markov decision processes. *Advances in Neural Information Processing Systems*, 35:28790–28802, 2022.

[Wang *et al.*, 2021] Jane X. Wang, Michael King, Nicolas Porcel, Zeb Kurth-Nelson, Tina Zhu, Charlie Deck, Peter Choy, Mary Cassin, Malcolm Reynolds, H. Francis Song, Gavin Buttimore, David P. Reichert, Neil C. Rabinowitz, Loic Matthey, Demis Hassabis, Alexander Lerchner, and Matthew M. Botvinick. Alchemy: A structured task distribution for meta-reinforcement learning. *CoRR*, abs/2102.02926, 2021.

[Watkins and Dayan, 1992] Christopher J. C. H. Watkins and Peter Dayan. Q-learning. *Machine Learning*, 8(3):279–292, May 1992.

[Xu and Mannor, 2010] Huan Xu and Shie Mannor. Distributionally robust markov decision processes. *Advances in Neural Information Processing Systems*, 23, 2010.

[Yu *et al.*, 2019] Tianhe Yu, Deirdre Quillen, Zhanpeng He, Ryan Julian, Karol Hausman, Chelsea Finn, and Sergey Levine. Meta-world: A benchmark and evaluation for multi-task and meta reinforcement learning. *CoRR*, abs/1910.10897, 2019.

[Zhu *et al.*, 2020] Yuke Zhu, Josiah Wong, Ajay Mandlekar, and Roberto Martín-Martín. robosuite: A modular simulation framework and benchmark for robot learning. *CoRR*, abs/2009.12293, 2020.

A Domains

We present details for the ATARI PacMan, Pong and Breakout domains.

A.1 PacMan

PacMan is set in a two-dimensional grid that contains food, walls, ghosts, and the PacMan character. The game concludes with a +500 reward when all food pellets are consumed, while encountering a ghost results in a -500 penalty and game over. Each consumed food pellet awards +10 points, and PacMan incurs a -1 penalty for every time step. The available actions for PacMan are moving Up, Down, Right, or Left. The game's state includes the location of PacMan, the position and direction of any ghosts, and the distribution of food pellets. In this iteration of the game, ghosts move according to some distributions.

A.2 Pong

In this one-player version of Pong, the player competes against a computer-controlled paddle. The game is set on a two-dimensional grid, with the player controlling one paddle and the computer controlling the other. The game concludes with a +500 reward when the ball reaches the grid boundaries on the computer controlled paddle side, while if the grid boundary is reached on the agent's side, a -500 penalty is applied and game over. The agent incurs a -1 penalty for every time step. The available actions for the paddles are moving Right and Left or to Stop. The game's state includes the location of the ball and the position and direction of any paddle. In this iteration of the game, the computer controlled paddle moves according to some distribution. Visualizations of the grids are presented in Sup1.

A.3 Breakout

In this version of Breakout, the agent competes against a wall of bricks using a horizontally-moving paddle and a ball. The game is set on a two-dimensional grid, with the agent controlling the paddle located at the bottom of the screen. The objective is to break bricks by hitting them with the ball, which bounces back after each hit. The game concludes with a +500 reward when all bricks are destroyed, but if the ball passes the paddle and reaches the bottom grid boundary, a -500 penalty is applied, resulting in game over. Each hit brick awards +10 points, and the agent incurs a -1 penalty for every time step. The available actions for the agent's paddle are moving Right or Left, or choosing to Stop. The game's state includes the position of the ball, the location of the paddle, and the configuration and status of the bricks. Visualizations of the grids are presented in Sup2.

B Training Parameters

In our experiments, parameters for Q-Learning and SARSA are inherited by [Cederborg *et al.*, 2015]. In particular, $\mathcal{T} = 1.5$ $\alpha = 0.05$, and $\lambda = 0.9$.

C Additional graphs showing the Generalization Agent outperforming the Learnability Agent in Non-Semantic variations

This section presents supplementary results showing the Generalization Agent and Learnability Agent behavior for Non-Semantic variations of grids throughout the analyzed domains.

C.1 PacMan

Additional results showing the Generalization Agent and Learnability Agent behaviour in Pacman for grids *v2*, *v3*, *v4*, are presented in the Supplementary figures. In particular, results for SARSA Agent with Boltzmann exploration strategy are presented in Sup3. Sup4, Sup5 show Q-learning Agent with Boltzmann and ϵ-greedy exploration strategies respectively.

C.2 Pong

Similarly, for Pong grids *p1*, *p2* results are presented in the Supplementary figures Sup6 for SARSA Agent and Sup7, Sup8 for Q-learning Agent.

C.3 Breakout

Analogously, for Breakout grids *b1*, *b2*, *b3* results are presented in the Supplementary figures Sup9, Sup10 for SARSA Agent and Sup11, Sup12 for Q-learning Agent.

D Additional graphs showing the Generalization Agent outperforming the Learnability Agent in Semantic variations

In this section we present supplementary results showing the Generalization Agent and Learnability Agent behavior for Semantic variations of grids throughout Pacman and Pong.

D.1 PacMan

The behavior of the Generalization and Learnabilty Agents under semantic variations of PacMan on grids *v2*, *v3*, *v4* are presented in Supplementary figures Sup13 for SARSA Agent and Sup14 and Sup15 for Q-learning Agent.

D.2 Pong

Similarly, for Pong grids p1, p2 results are presented in the Supplementary figures. In particular, semantic variations featuring Directional Ghost $p = 0.3$ are presented in Sup16, Sup17 for SARSA Agent and Sup18, Sup19 for Q-learning Agent. While semantic variations featuring Directional Ghost $p = 0.6$ are shown in Sup20, Sup21 for SARSA Agent and Sup22, Sup23 for Q-learning.

E Additional graphs showing patterns of state-action pairs

This section shows the supplementary results for the *exploration grid* visualizing the difference in State-Action (S-A) pairs explored by these agents (D_{LG}) throughout the analyzed domains.

E.1 PacMan

Results of the *exploration grid* for PacMan *v2*, *v3*, *v4* are shown in Supplementary figures. In particular, for non-semantic grid variations, Sup24 and Sup25 report grid exploration graphs for Q-learning Agent and Sup26 and Sup27 for SARSA Agent. Additionally, for semantic games variations, Sup28 and Sup29 report grid exploration graphs for Q-learning Agent and Sup30 and Sup31 for SARSA Agent.

E.2 Pong

Similarly, for pong *p1* and *p2*, Sup32, Sup33, Sup34, and Sup35 report grid exploration graphs for non-semantic variations of Q-learning Agent and SARSA Agent respectively, while Sup36, Sup37, Sup38, and Sup39 for semantic variations.

E.3 Breakout

For Breakout grids *b1*,*b2*, and *b3*, exploration graphs for non-semantic variations of Q-learning Agent and SARSA Agent are reported in Supplementary figures Sup40, Sup41, Sup42, and Sup43.

Pong

p1

p2
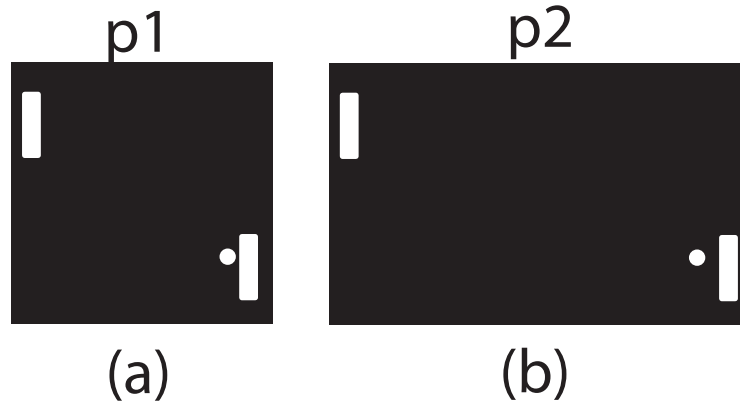
Figure Sup1: *Grid variations for Pong.*

Breakout

b1

b2

b3
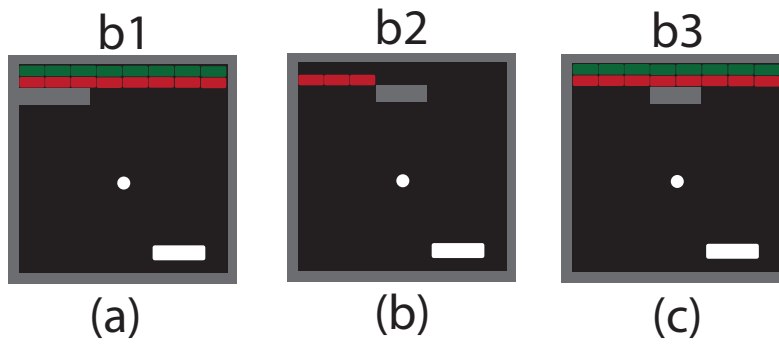
Figure Sup2: *Grid variations for Breakout.*
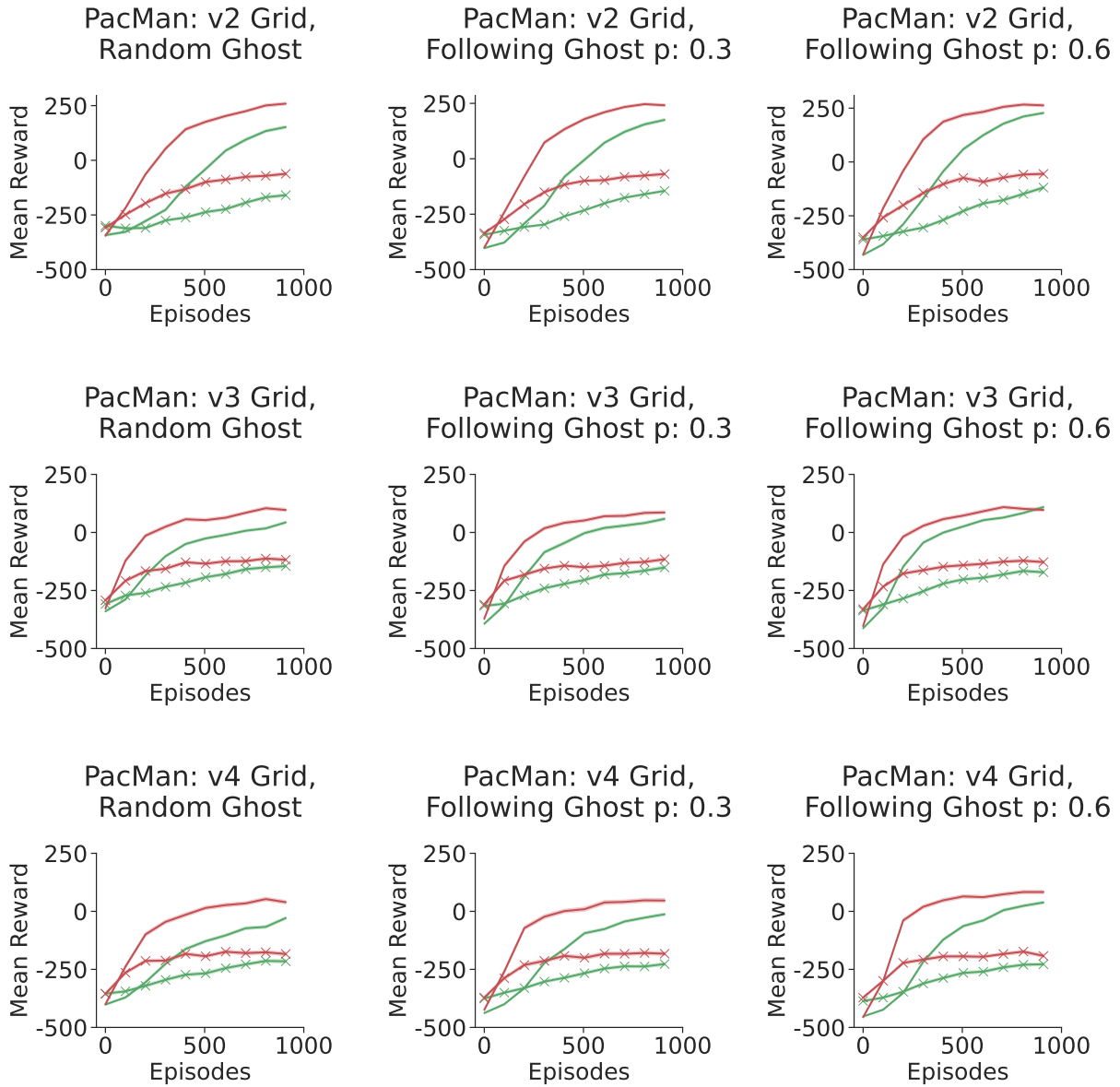
Figure Sup3: *SARSA Agent with Boltzmann exploration strategy*: Results for PacMan v2, v3, v4 grids reporting mean reward as a function of episode number. The agent is trained on the non-noisy version of the environment and tested on different level of noise ($\delta \sim \mathcal{N}(0, 0.1)$ in Low-Noise and $\delta \sim \mathcal{N}(0, 0.5)$ in High-Noise settings).
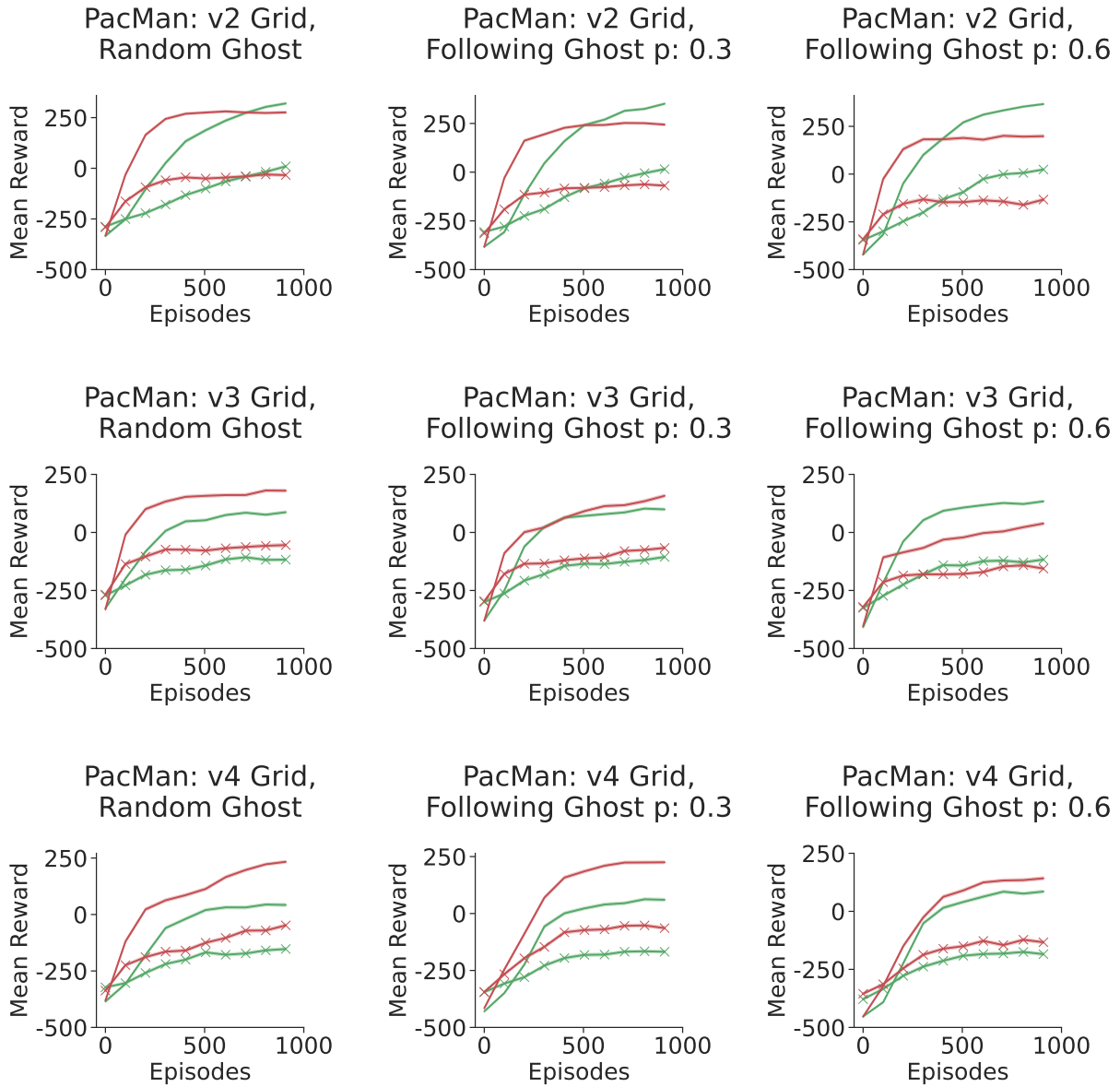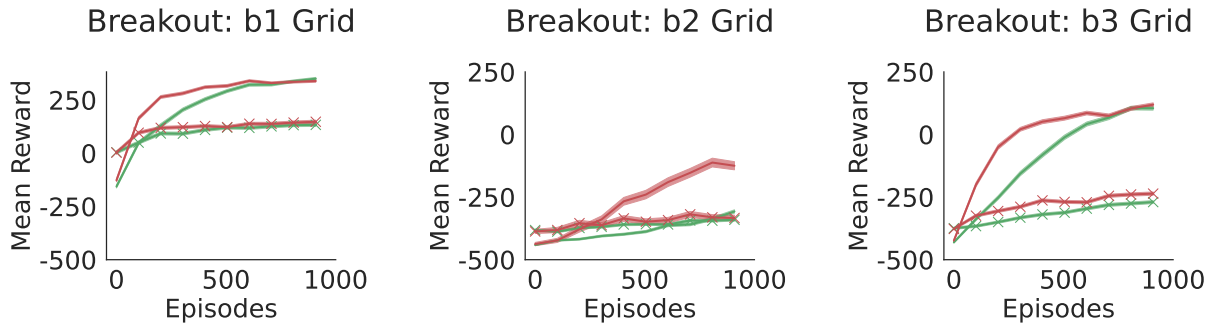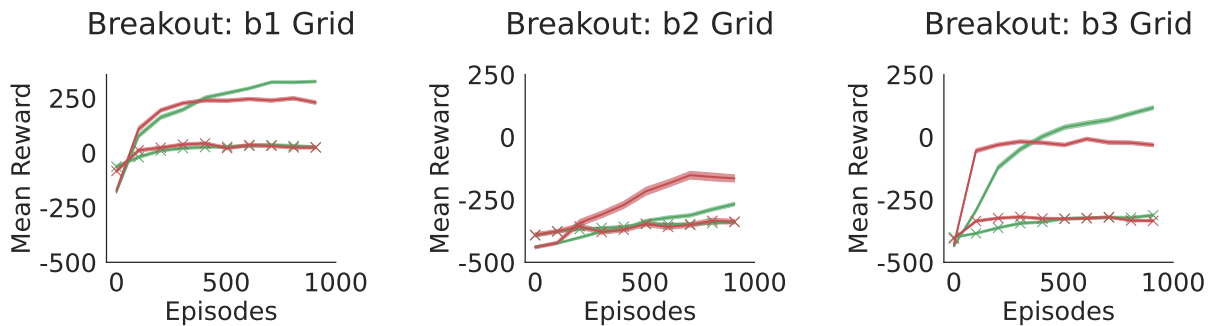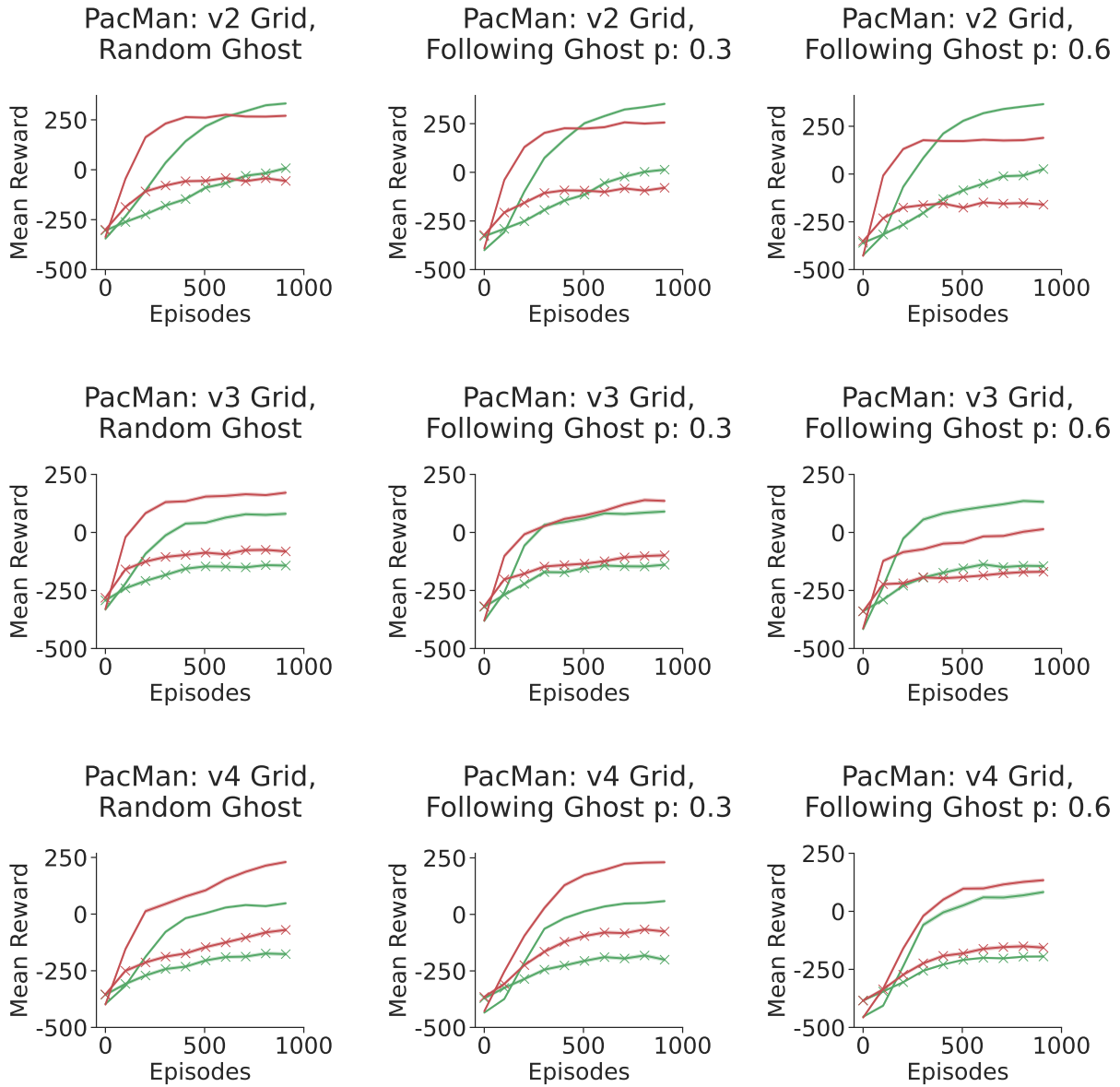
Figure Sup4: *Q-learning Agent with Boltzmann exploration strategy*: Results for PacMan v2, v3, v4 grids reporting mean reward as a function of episode number. The agent is trained on the non-noisy version of the environment and tested on different level of noise ($\delta \sim \mathcal{N}(0, 0.1)$ in Low-Noise and $\delta \sim \mathcal{N}(0, 0.5)$ in High-Noise settings).
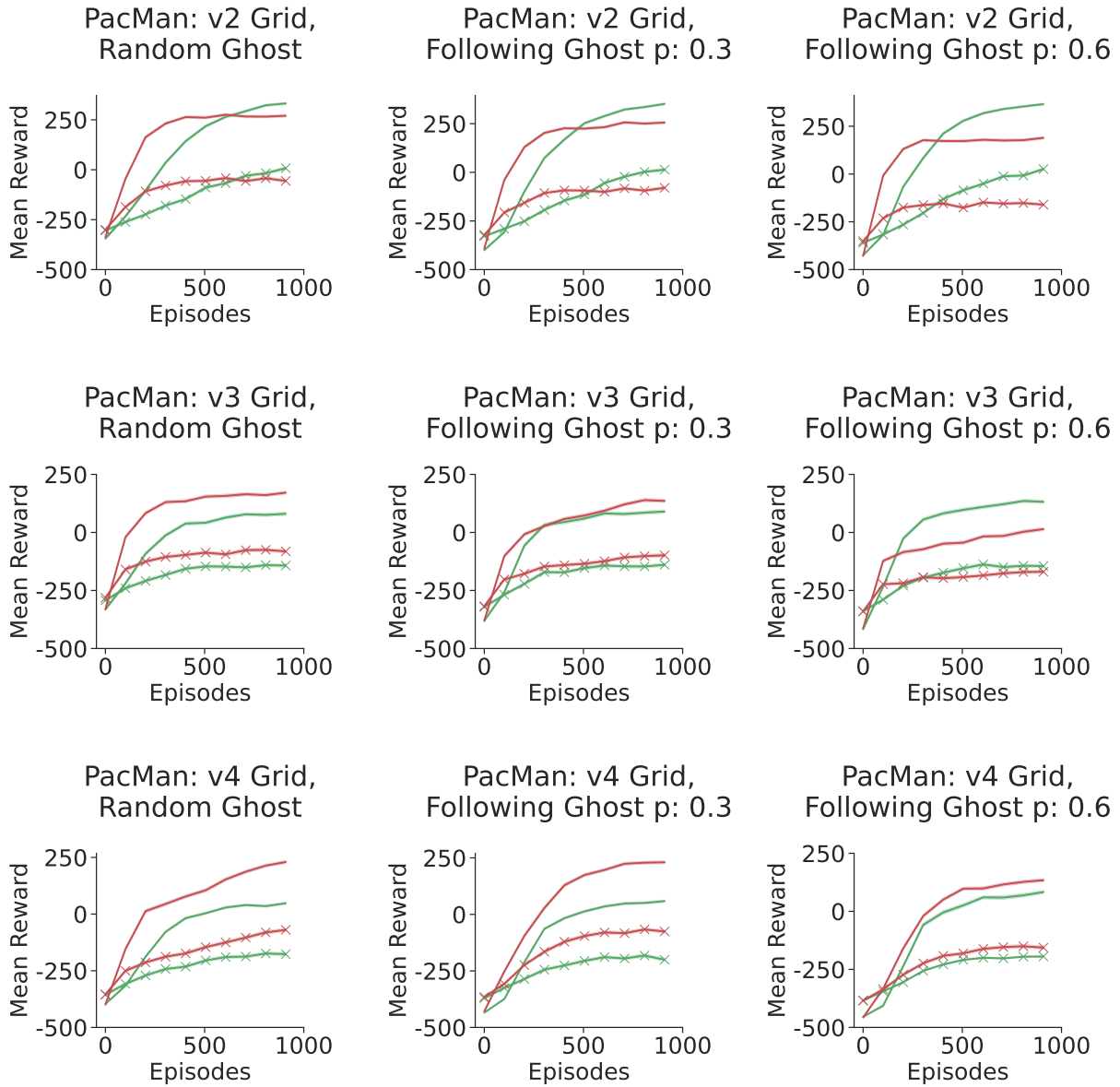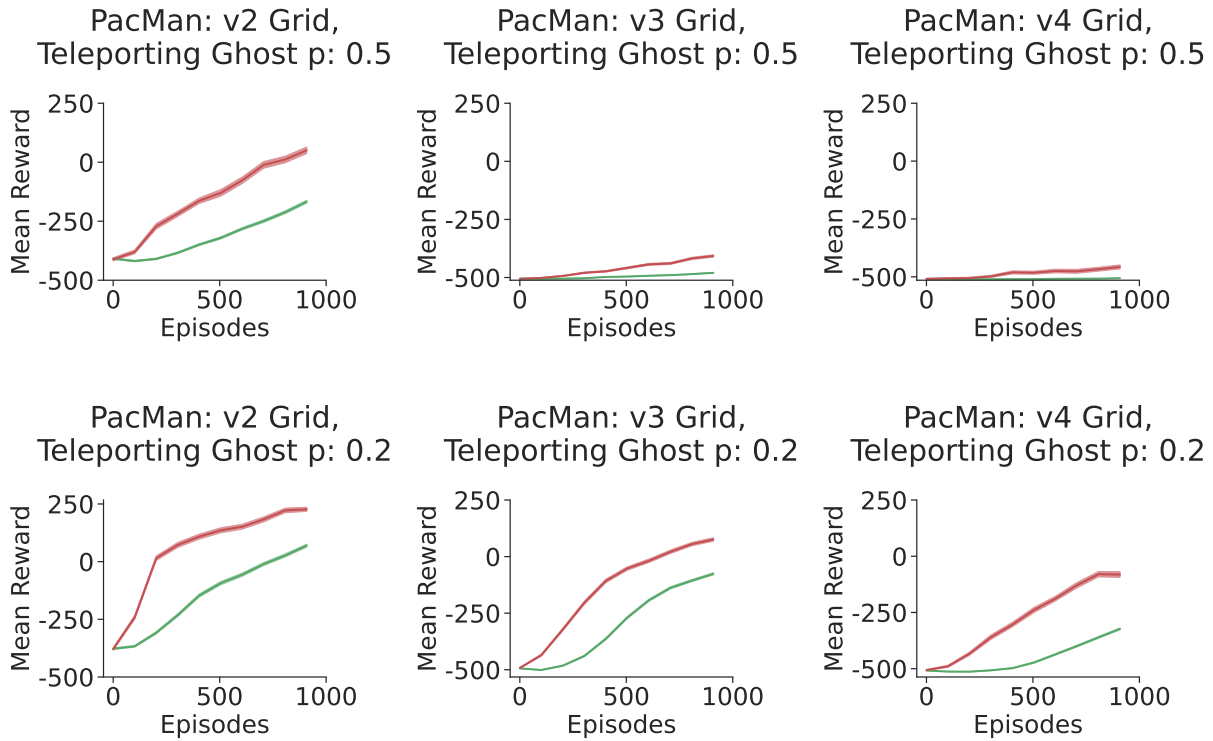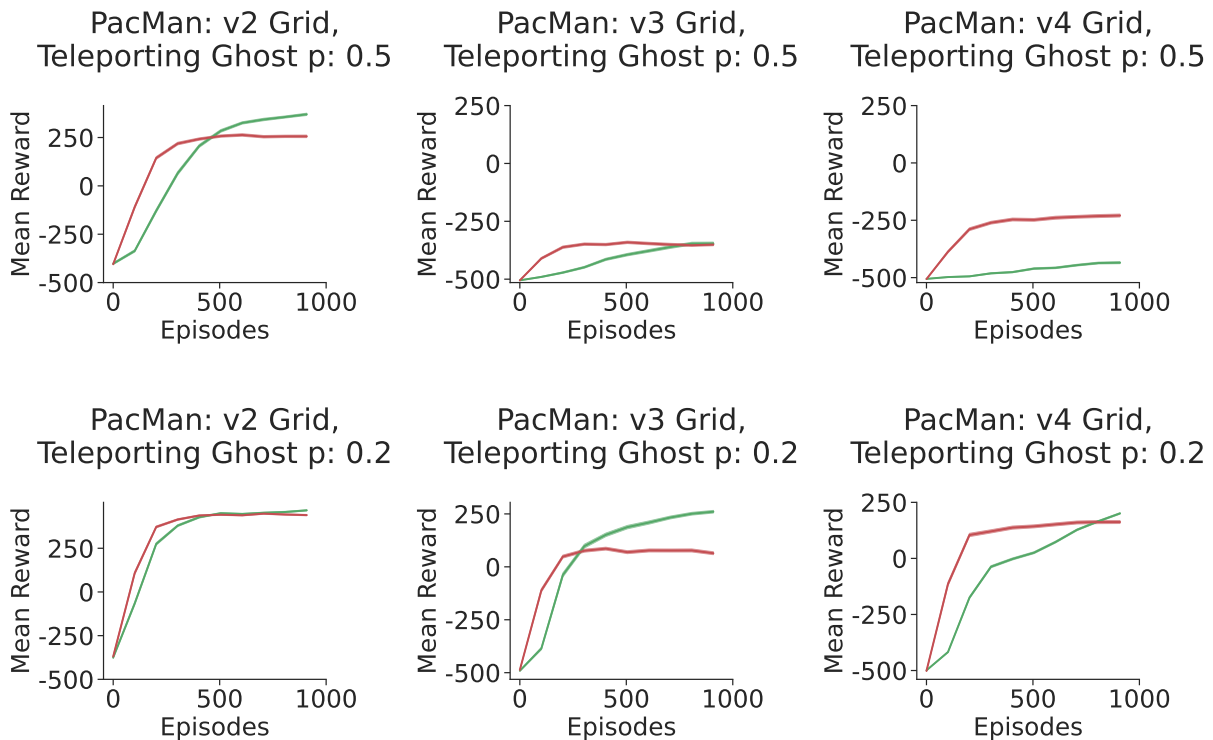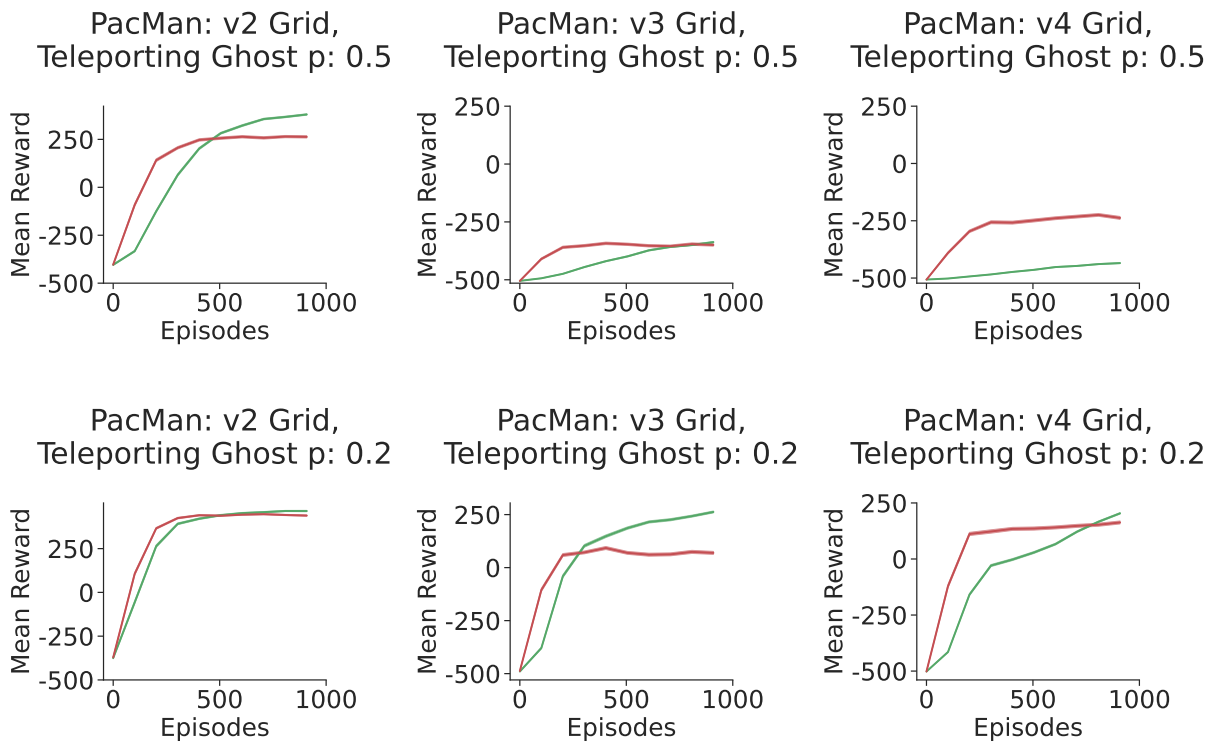
Figure Sup5: *Q-learning Agent with ε-greedy exploration strategy*: Results for PacMan v2, v3, v4 grids reporting mean reward as a function of episode number. The agent is trained on the non-noisy version of the environment and tested on different level of noise ($δ \sim \mathcal{N}(0, 0.1)$ in Low-Noise and $δ \sim \mathcal{N}(0, 0.5)$ in High-Noise settings).
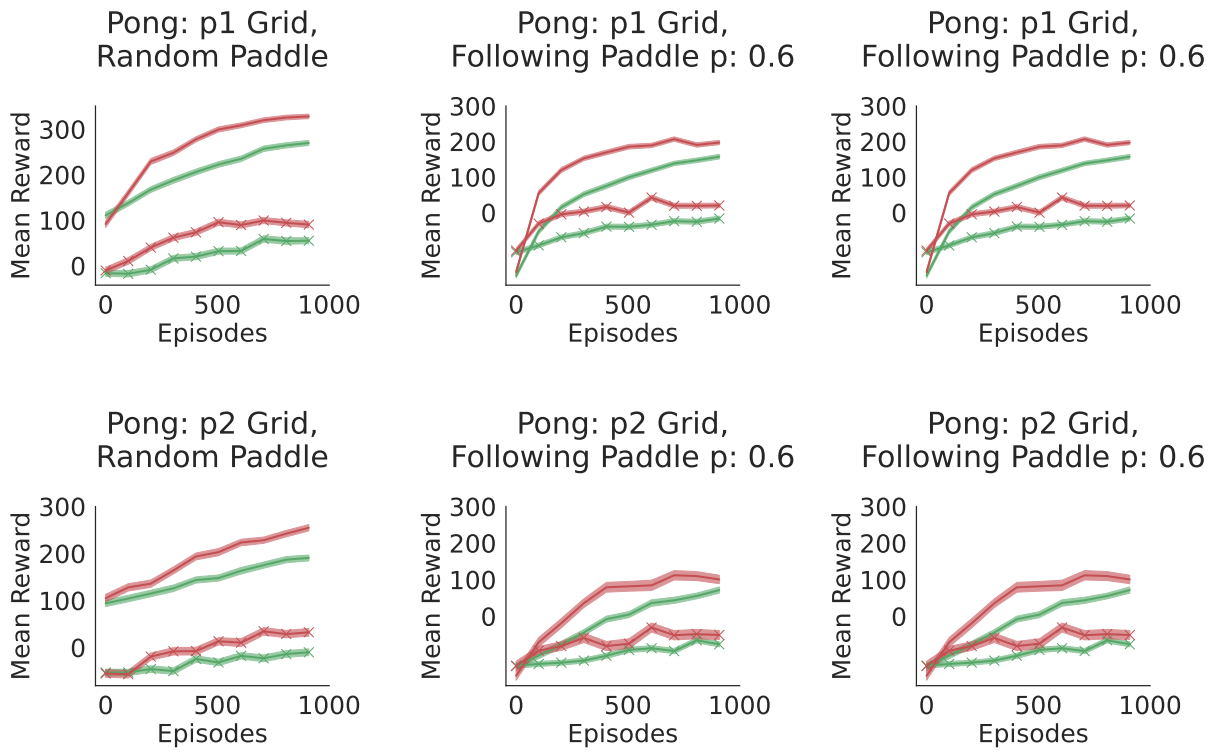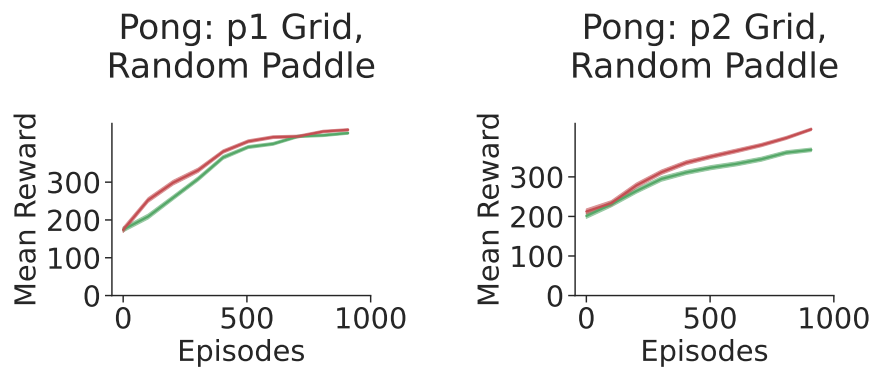
Figure Sup6: *SARSA Agent with Boltzmann exploration strategy*: Results for Pong p1, p2 grids reporting mean reward as a function of episode number. The agent is trained on the non-noisy version of the environment and tested on different level of noise ($\delta \sim \mathcal{N}(0, 0.1)$ in Low-Noise and $\delta \sim \mathcal{N}(0, 0.5)$ in High-Noise settings).
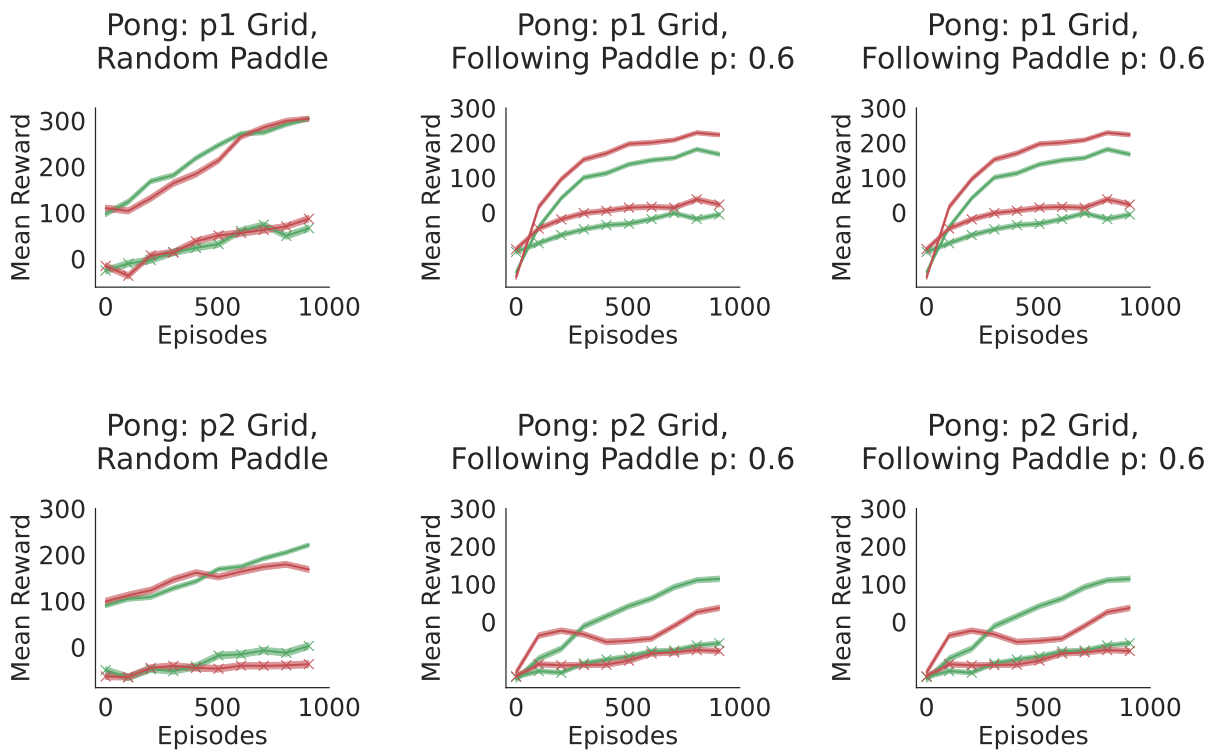
Figure Sup7: *Q-learning Agent with Boltzmann exploration strategy*: Results for Pong p1, p2 grids reporting mean reward as a function of episode number. The agent is trained on the non-noisy version of the environment and tested on different level of noise ($\delta \sim \mathcal{N}(0, 0.1)$ in Low-Noise and $\delta \sim \mathcal{N}(0, 0.5)$ in High-Noise settings).
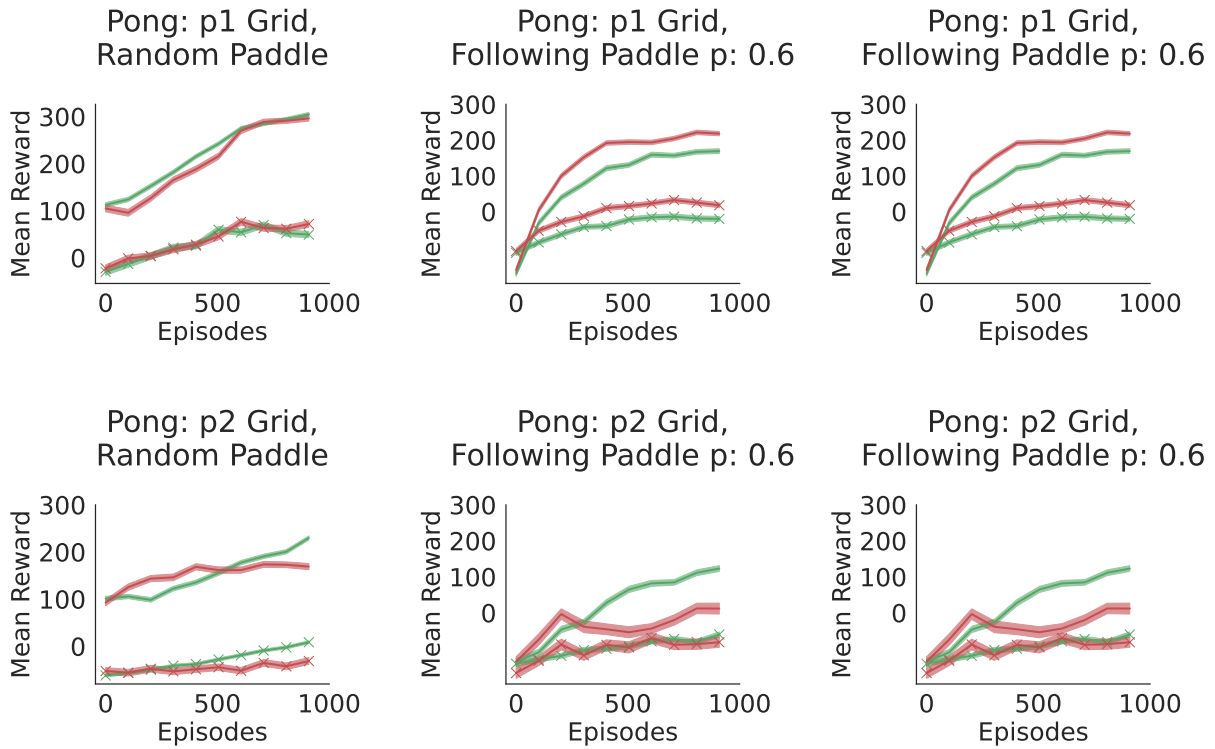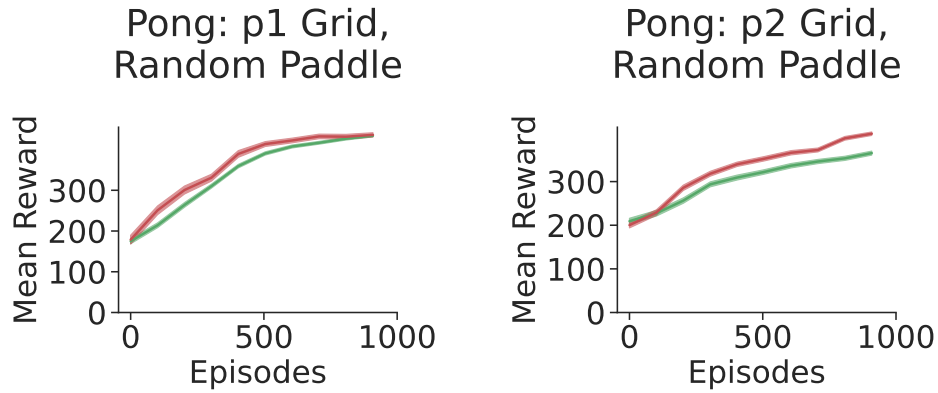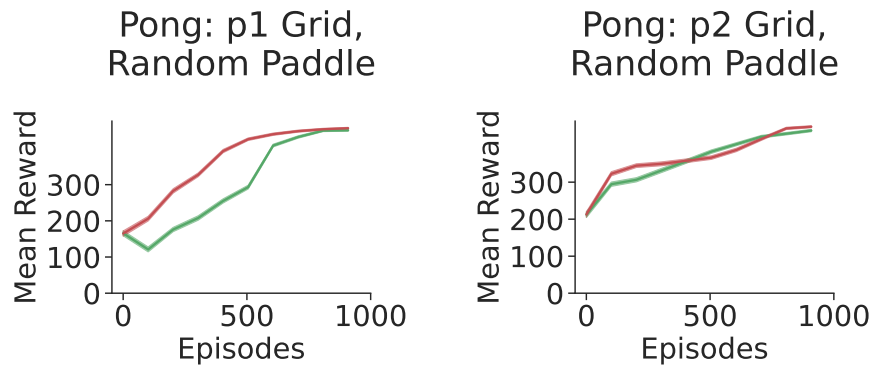
Figure Sup8: *Q-learning Agent with ε-greedy exploration strategy*: Results for Pong p1, p2 grids reporting mean reward as a function of episode number. The agent is trained on the non-noisy version of the environment and tested on different level of noise ($\delta \sim \mathcal{N}(0, 0.1)$ in Low-Noise and $\delta \sim \mathcal{N}(0, 0.5)$ in High-Noise settings).
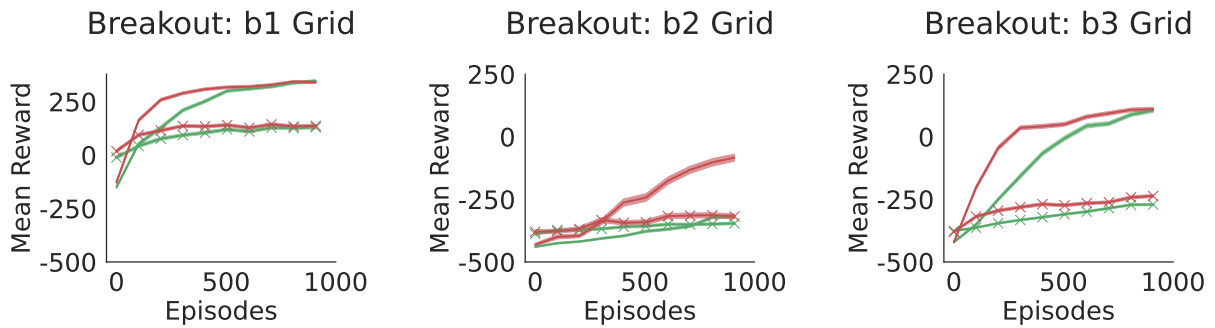
Figure Sup9: *SARSA Agent with Boltzmann exploration strategy*: Results for Breakout b1, b2, b3 grids reporting mean reward as a function of episode number. The agent is trained on the non-noisy version of the environment and tested on different level of noise ($\delta \sim \mathcal{N}(0, 0.1)$ in Low-Noise and $\delta \sim \mathcal{N}(0, 0.5)$ in High-Noise settings).

Figure Sup10: *SARSA Agent with ε-greedy exploration strategy*: Results for Breakout b1, b2, b3 grids reporting mean reward as a function of episode number. The agent is trained on the non-noisy version of the environment and tested on different level of noise ($\delta \sim \mathcal{N}(0, 0.1)$ in Low-Noise and $\delta \sim \mathcal{N}(0, 0.5)$ in High-Noise settings).

Figure Sup11: *Q-learning Agent with Boltzmann exploration strategy*: Results for Breakout b1, b2, b3 grids reporting mean reward as a function of episode number. The agent is trained on the non-noisy version of the environment and tested on different level of noise ($\delta \sim \mathcal{N}(0, 0.1)$ in Low-Noise and $\delta \sim \mathcal{N}(0, 0.5)$ in High-Noise settings).
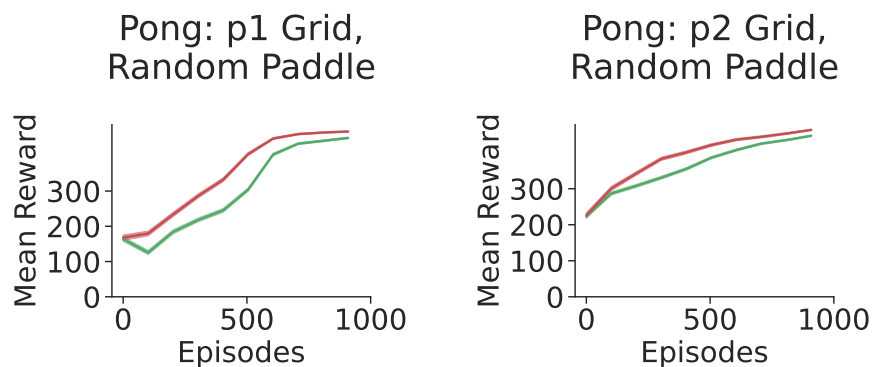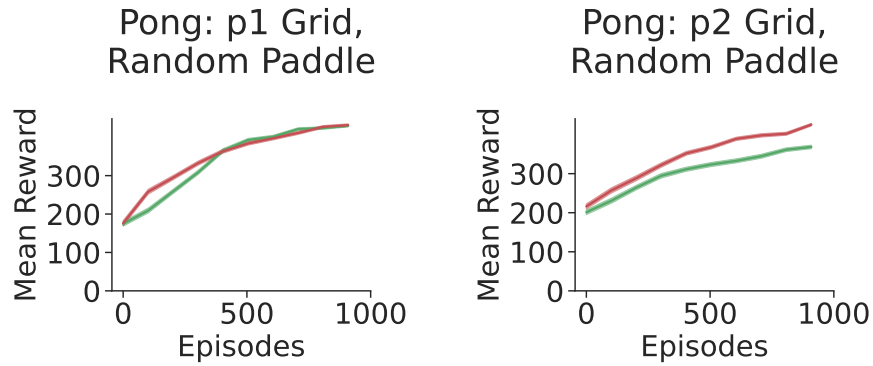
Figure Sup12: *Q-learning Agent with ϵ-greedy exploration strategy* Results for Pong p1, p2 grids reporting mean reward as a function of episode number. The agent is trained on the non-noisy version of the environment and tested on different level of noise ($\delta \sim \mathcal{N}(0, 0.1)$ in Low-Noise and $\delta \sim \mathcal{N}(0, 0.5)$ in High-Noise settings).

Figure Sup13: *SARSA Agent with Boltzmann exploration strategy*: Results for PacMan v2, v3, v4 grids reporting mean reward as a function of episode number. The agent is trained on the Random Ghost environment and tested on the Teleporting Ghost variation ($p = 0.2$, $p = 0.5$)
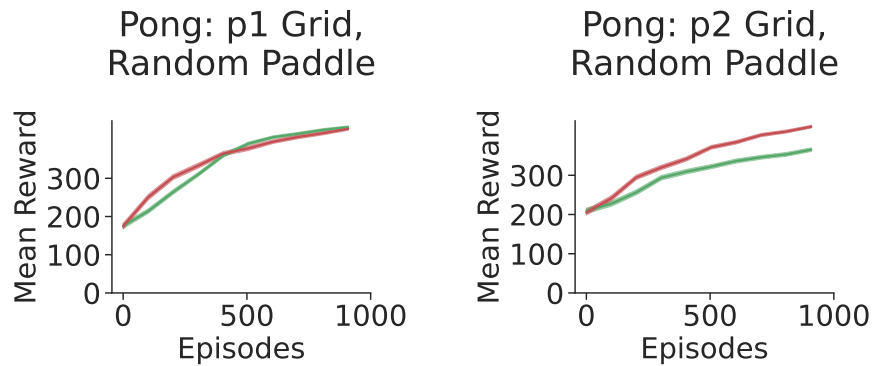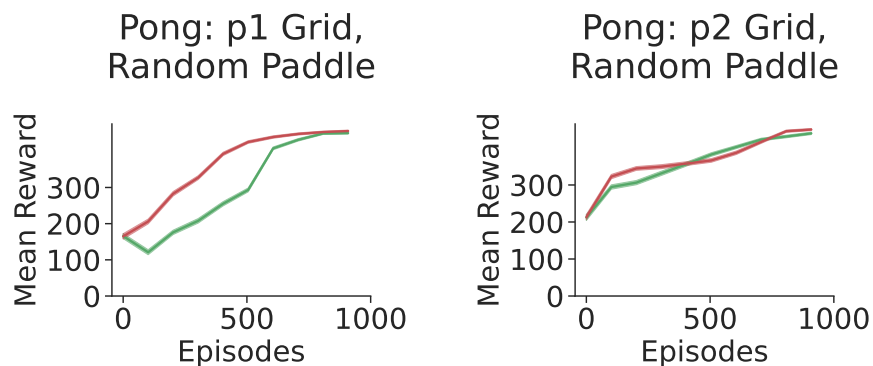

Figure Sup14: *Q-learning Agent with Boltzmann exploration strategy*: Results for PacMan v2, v3, v4 grids reporting mean reward as a function of episode number. The agent is trained on the Random Ghost environment and tested on the Teleporting Ghost variation ($p = 0.2$, $p = 0.5$)

Figure Sup15: *Q-learning Agent with ε-greedy exploration strategy*: Results for PacMan v2, v3, v4 grids reporting mean reward as a function of episode number. The agent is trained on the Random Ghost environment and tested on the Teleporting Ghost variation ($p = 0.2$, $p = 0.5$)

Figure Sup16: *SARSA Agent with Boltzmann exploration strategy*: Results for Pong p1, p2 grids reporting mean reward as a function of episode number. The agent is trained on the Directional Ghost ($p = 0.3$) environment and tested on the Random Ghost variation.
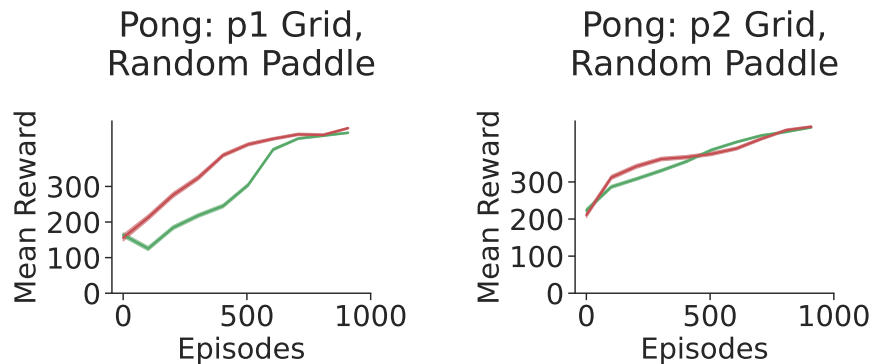
Pong: p1 Grid,
Random Paddle

Pong: p2 Grid,
Random Paddle

Figure Sup17: *SARSA Agent with ε-greedy exploration strategy*: Results for Pong p1, p2 grids reporting mean reward as a function of episode number. The agent is trained on the Directional Ghost ($p = 0.3$) environment and tested on the Random Ghost variation.

Pong: p1 Grid,
Random Paddle

Pong: p2 Grid,
Random Paddle

Figure Sup18: *Q-learning Agent with Boltzmann exploration strategy*: Results for Pong p1, p2 grids reporting mean reward as a function of episode number. The agent is trained on the Directional Ghost ($p = 0.3$) environment and tested on the Random Ghost variation.

Pong: p1 Grid,
Random Paddle

Pong: p2 Grid,
Random Paddle

Figure Sup19: *Q-learning Agent with ε-greedy exploration strategy*: Results for Pong p1, p2 grids reporting mean reward as a function of episode number. The agent is trained on the Directional Ghost ($p = 0.3$) environment and tested on the Random Ghost variation.

Pong: p1 Grid, Random Paddle

Pong: p2 Grid, Random Paddle

Figure Sup20: *SARSA Agent with Boltzmann exploration strategy*: Results for Pong p1, p2 grids reporting mean reward as a function of episode number. The agent is trained on the Directional Ghost ($p = 0.3$) environment and tested on the Random Ghost variation.

Pong: p1 Grid, Random Paddle

Pong: p2 Grid, Random Paddle

Figure Sup21: *SARSA Agent with ϵ-greedy exploration strategy*: Results for Pong p1, p2 grids reporting mean reward as a function of episode number. The agent is trained on the Directional Ghost ($p = 0.3$) environment and tested on the Random Ghost variation.

Pong: p1 Grid, Random Paddle

Pong: p2 Grid, Random Paddle

Figure Sup22: *Q-learning Agent with Boltzmann exploration strategy*: Results for Pong p1, p2 grids reporting mean reward as a function of episode number. The agent is trained on the Directional Ghost ($p = 0.3$) environment and tested on the Random Ghost variation.

Figure Sup23: *Q-learning Agent with ϵ-greedy exploration strategy*: Results for Pong p1, p2 grids reporting mean reward as a function of episode number. The agent is trained on the Directional Ghost ($p = 0.3$) environment and tested on the Random Ghost variation.
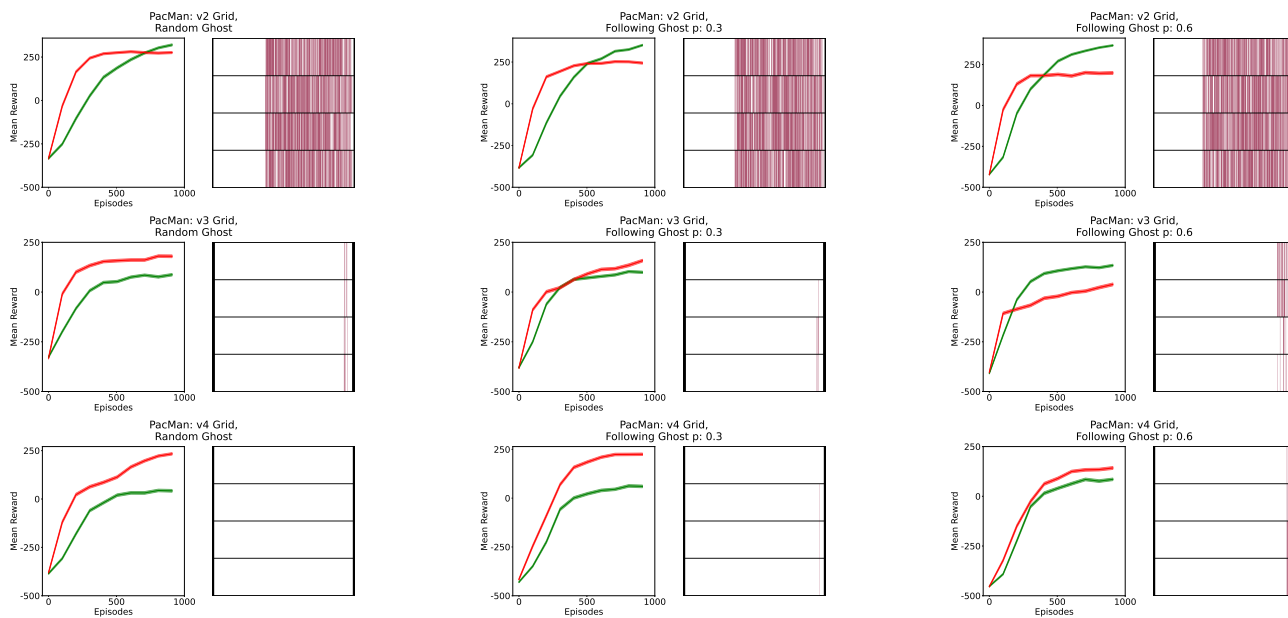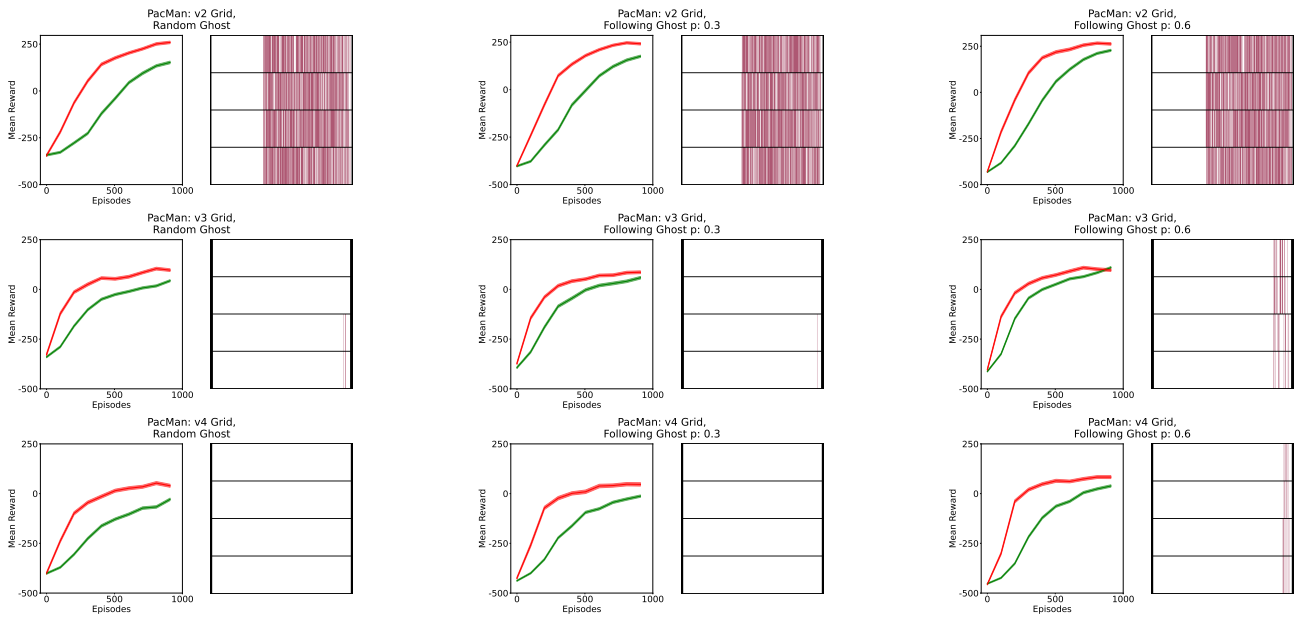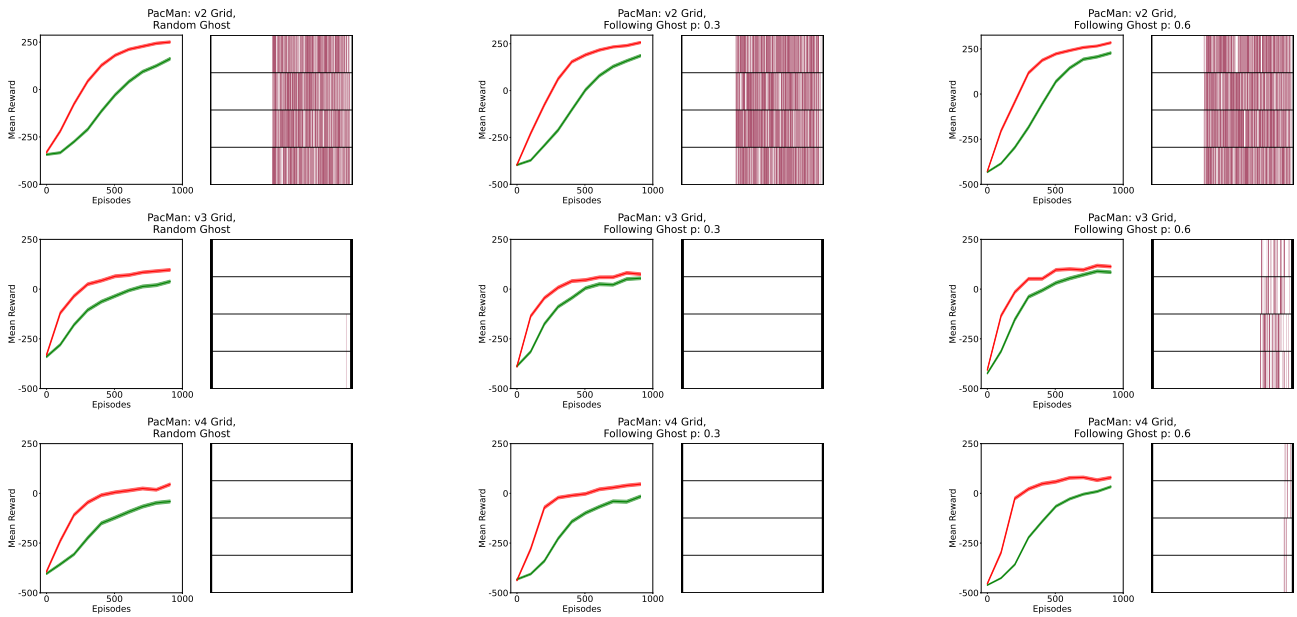

Figure Sup24: *Q-learning Agent with Boltzmann exploration strategy*: The *exploration grid* visualizing the difference in State-Action (S-A) pairs explored by these agents (D_{LG}). Results for PacMan v2, v3, v4 grids, the agent is trained on non-noisy variations of different environments (reported in the headings) and tested in the Low-Noise regime. Rows in the right figure represents agent's actions Left, Right, Up, or Down.
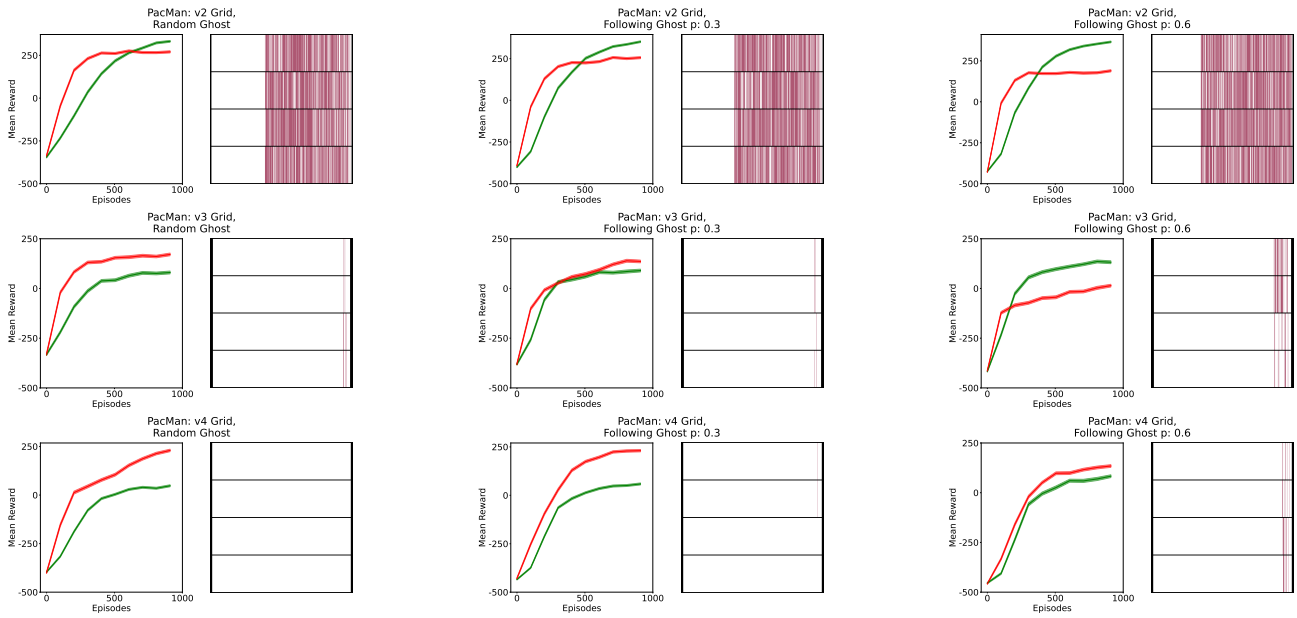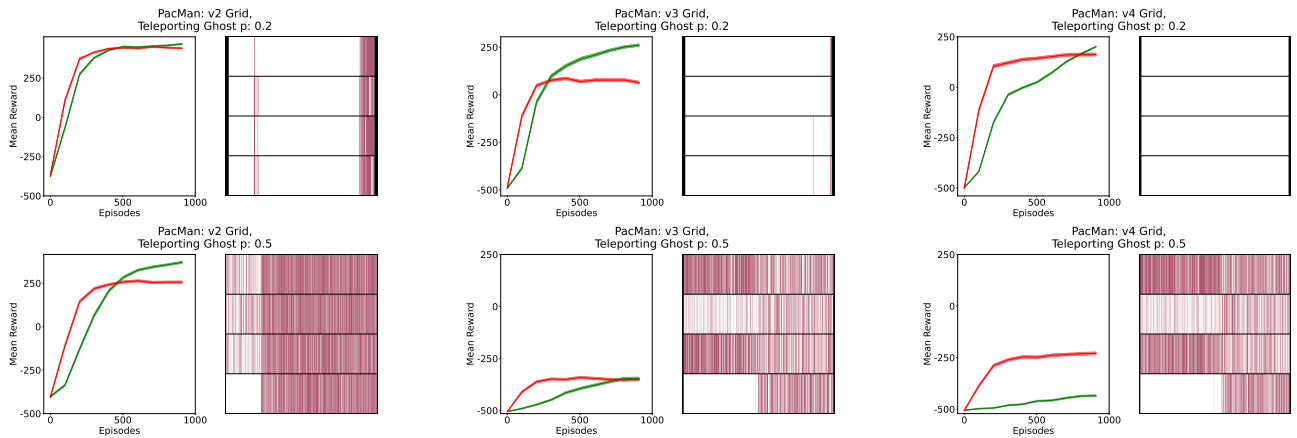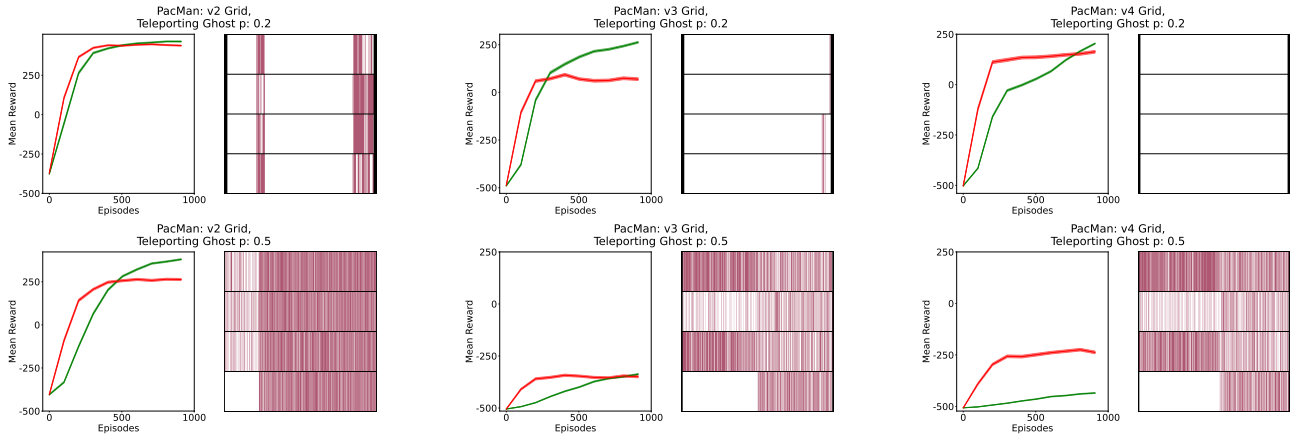
Figure Sup25: *Q-learning Agent with ϵ-greedy exploration strategy*: The *exploration grid* visualizing the difference in State-Action (S-A) pairs explored by these agents (D_{LG}). Results for PacMan v2, v3, v4 grids, the agent is trained on non-noisy variations of different environments (reported in the headings) and tested in the Low-Noise regime. Rows in the right figure represents agent's actions Left, Right, Up, or Down.
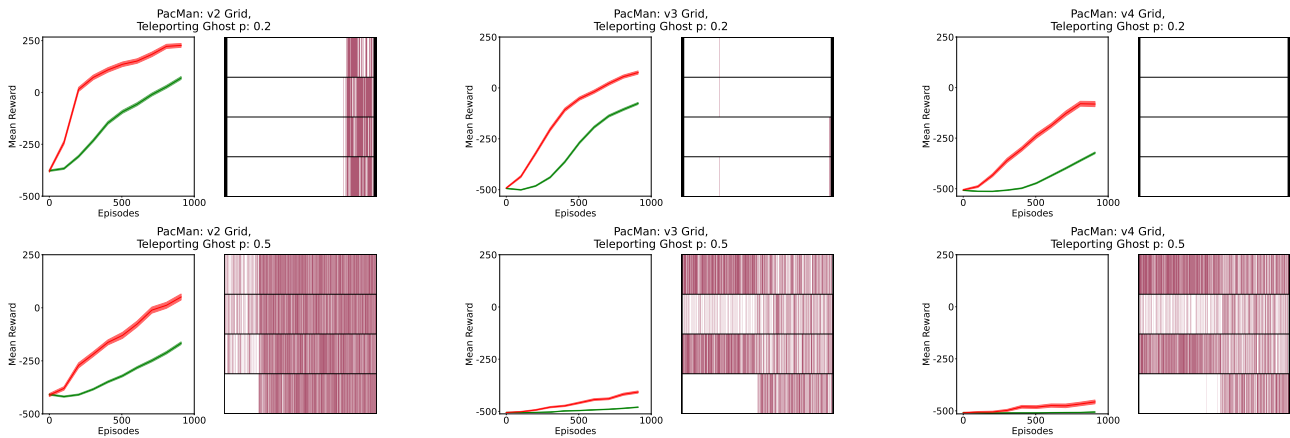

Figure Sup26: *SARSA Agent with Boltzmann exploration strategy*: The *exploration grid* visualizing the difference in State-Action (S-A) pairs explored by these agents (D_{LG}). Results for PacMan v2, v3, v4 grids, the agent is trained on non-noisy variations of different environments (reported in the headings) and tested in the Low-Noise regime. Rows in the right figure represents agent's actions Left, Right, Up, or Down.

Figure Sup27: *SARSA Agent with ε-greedy exploration strategy*: The *exploration grid* visualizing the difference in State-Action (S-A) pairs explored by these agents (D_{LG}). Results for PacMan v2, v3, v4 grids, the agent is trained on non-noisy variations of different environments (reported in the headings) and tested in the Low-Noise regime. Rows in the right figure represents agent's actions Left, Right, Up, or Down.

Figure Sup28: *Q-learning Agent with Boltzmann exploration strategy*: The *exploration grid* visualizing the difference in State-Action (S-A) pairs explored by these agents (D_{LG}). Results for PacMan v2, v3, v4 grids, the agent is trained on Teleporting Ghost variation ($p = 0.2$, $p = 0.5$) and tested in different environments (reported in the headings). Rows in the right figure represents agent's actions Left, Right, Up, or Down.
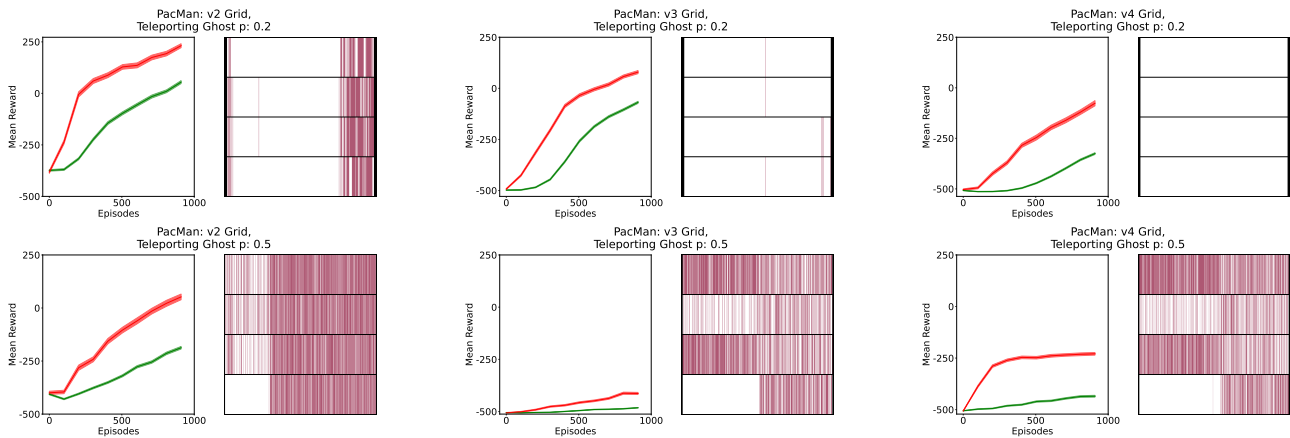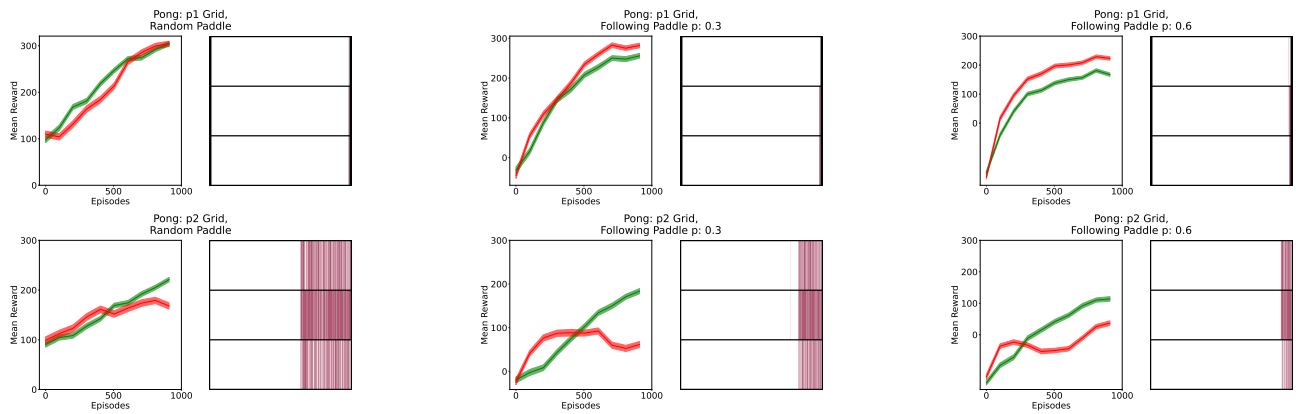
Figure Sup29: *Q-learning Agent with ε-greedy exploration strategy*: The *exploration grid* visualizing the difference in State-Action (S-A) pairs explored by these agents (D_{LG}). Results for PacMan v2, v3, v4 grids, the agent is trained on Teleporting Ghost variation ($p = 0.2$, $p = 0.5$) and tested in different environments (reported in the headings). Rows in the right figure represents agent's actions Left, Right, Up, or Down.

Figure Sup30: *SARSA Agent with Boltzmann exploration strategy*: The *exploration grid* visualizing the difference in State-Action (S-A) pairs explored by these agents (D_{LG}). Results for PacMan v2, v3, v4 grids, the agent is trained on Teleporting Ghost variation ($p = 0.2$, $p = 0.5$) and tested in different environments (reported in the headings). Rows in the right figure represents agent's actions Left, Right, Up, or Down.

Figure Sup31: *SARSA Agent with ε-greedy exploration strategy*: The *exploration grid* visualizing the difference in State-Action (S-A) pairs explored by these agents (D_{LG}). Results for PacMan v2, v3, v4 grids, the agent is trained on Teleporting Ghost variation ($p = 0.2$, $p = 0.5$) and tested in different environments (reported in the headings). Rows in the right figure represents agent's actions Left, Right, Up, or Down.

Figure Sup32: *Q-learning Agent with Boltzmann exploration strategy*: The *exploration grid* visualizing the difference in State-Action (S-A) pairs explored by these agents (D_{LG}). Results for Pong p1, p2 grids, the agent is trained on non-noisy variations of different environments (reported in the headings) and tested in the Low-Noise regime. Rows in the right figure represents agent's actions Left, Right, Stop.
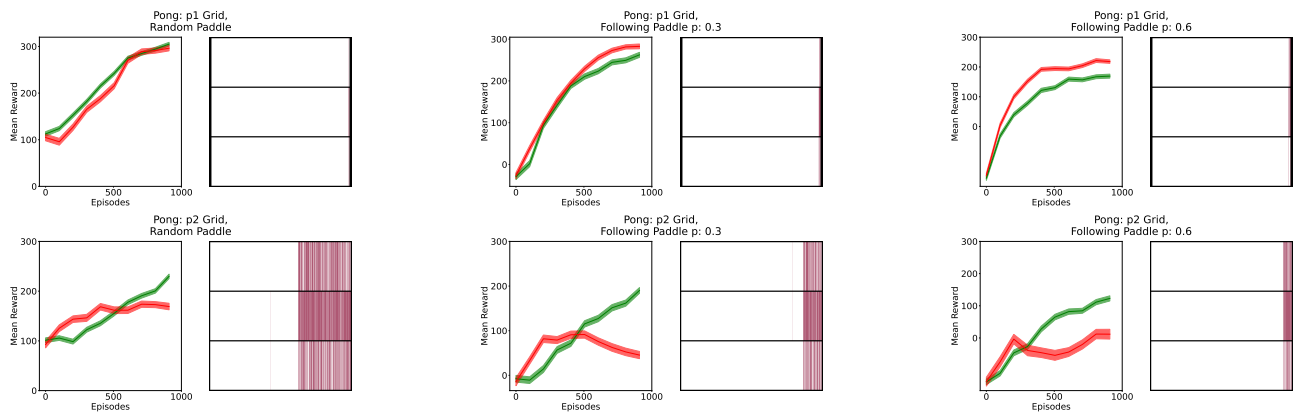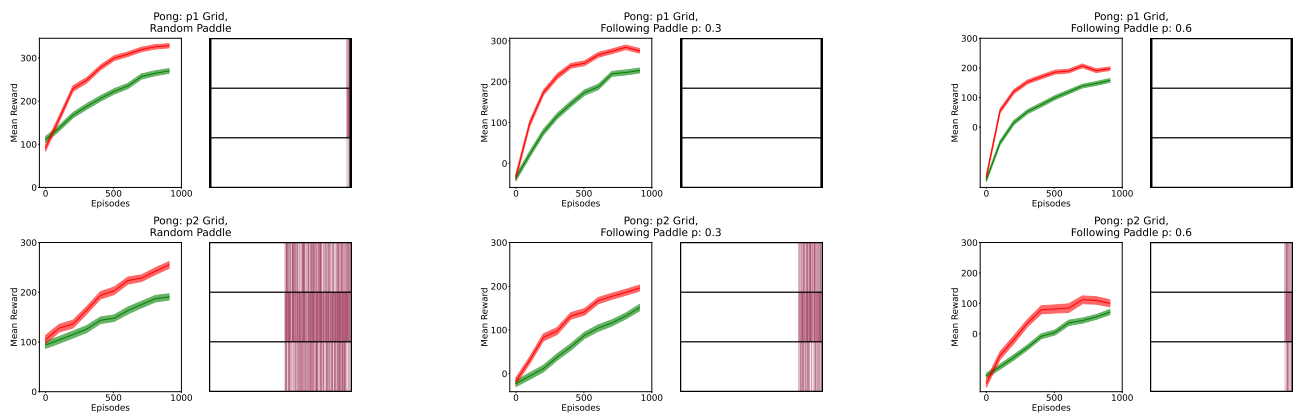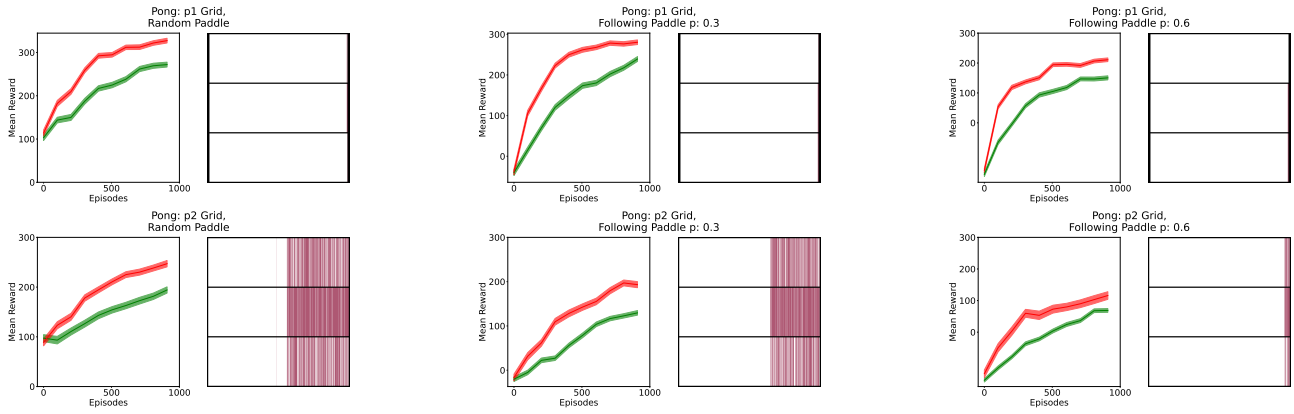

Figure Sup33: *Q-learning Agent with ϵ-greedy exploration strategy*: The *exploration grid* visualizing the difference in State-Action (S-A) pairs explored by these agents (D_{LG}). Results for Pong p1, p2 grids, the agent is trained on non-noisy variations of different environments (reported in the headings) and tested in the Low-Noise regime. Rows in the right figure represents agent's actions Left, Right, Stop.
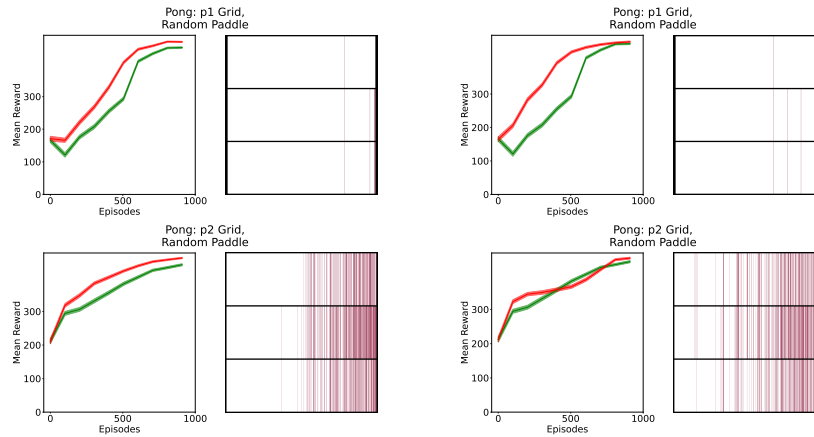

Figure Sup34: *SARSA Agent with Boltzmann exploration strategy*: The *exploration grid* visualizing the difference in State-Action (S-A) pairs explored by these agents (D_{LG}). Results for Pong p1, p2 grids, the agent is trained on non-noisy variations of different environments (reported in the headings) and tested in the Low-Noise regime. Rows in the right figure represents agent's actions Left, Right, Stop.

Figure Sup35: *SARSA Agent with ε-greedy exploration strategy*: The *exploration grid* visualizing the difference in State-Action (S-A) pairs explored by these agents (D_{LG}). Results for Pong p1, p2 grids, the agent is trained on non-noisy variations of different environments (reported in the headings) and tested in the Low-Noise regime. Rows in the right figure represents agent's actions Left, Right, Stop.

Figure Sup36: *Q-learning Agent with Boltzmann exploration strategy*: The *exploration grid* visualizing the difference in State-Action (S-A) pairs explored by these agents (D_{LG}). Results for Pong p1, p2 grids, the agent is trained on Directional paddle ($p = 0.3$ top, $p = 0.6$, bottom) variation and tested in the Random paddle environment. Rows in the right figure represents agent's actions Left, Right, Stop.
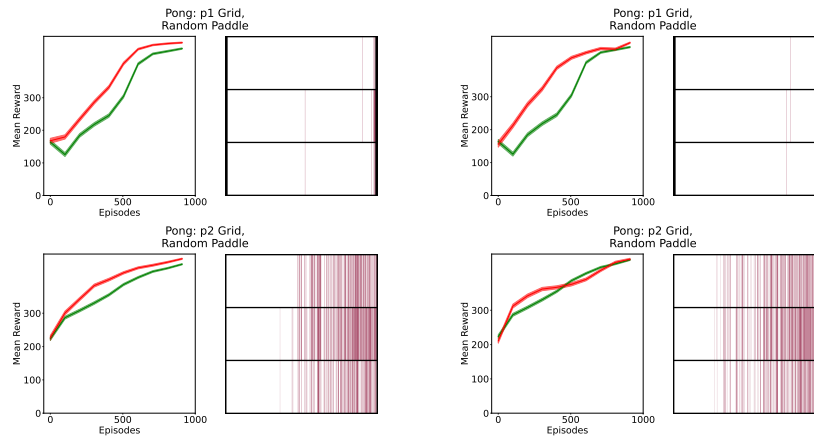

Figure Sup37: *Q-learning Agent with ε-greedy exploration strategy*: The *exploration grid* visualizing the difference in State-Action (S-A) pairs explored by these agents (D_{LG}). Results for Pong p1, p2 grids, the agent is trained on Directional Paddle ($p = 0.3$ top, $p = 0.6$, bottom) variation and tested in the Random Paddle environment. Rows in the right figure represents agent's actions Left, Right, Stop.
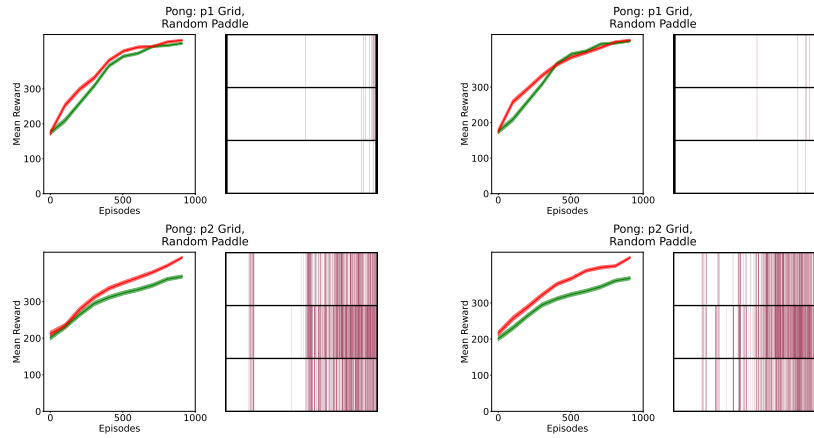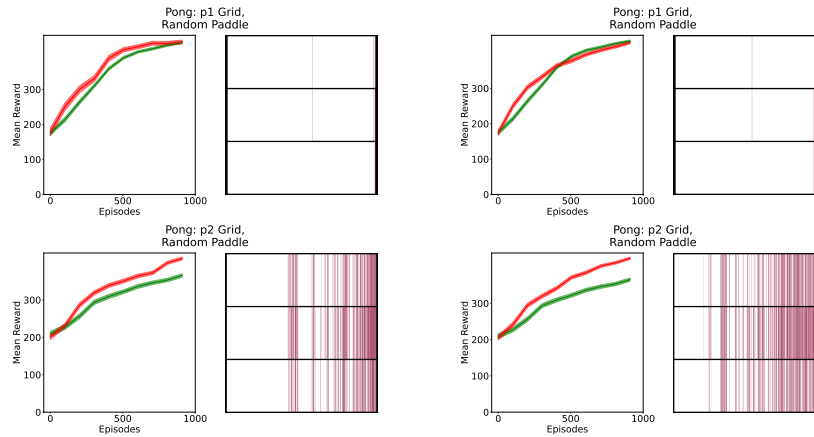
Figure Sup38: *SARSA Agent with Boltzmann exploration strategy*: The *exploration grid* visualizing the difference in State-Action (S-A) pairs explored by these agents (D_{LG}). Results for Pong p1, p2 grids, the agent is trained on Directional Paddle ($p = 0.3$ top, $p = 0.6$, bottom) variation and tested in the Random Paddle environment. Rows in the right figure represents agent's actions Left, Right, Stop.

Figure Sup39: *SARSA Agent with ϵ-greedy exploration strategy*: The *exploration grid* visualizing the difference in State-Action (S-A) pairs explored by these agents (D_{LG}). Results for Pong p1, p2 grids, the agent is trained on Directional Paddle ($p = 0.3$ top, $p = 0.6$, bottom) variation and tested in the Random Paddle environment. Rows in the right figure represents agent's actions Left, Right, Stop.
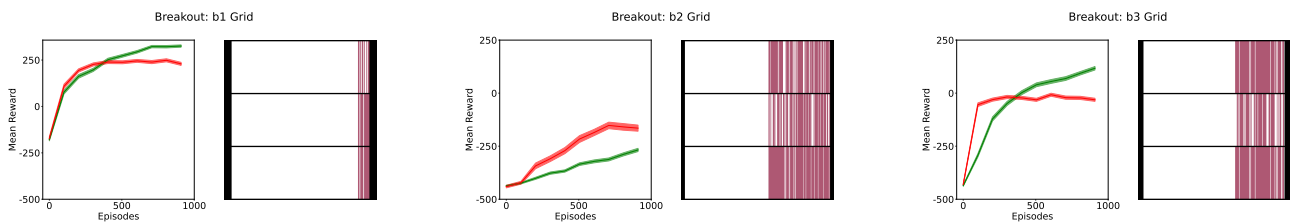

Figure Sup40: *Q-learning Agent with Boltzmann exploration strategy*: The *exploration grid* visualizing the difference in State-Action (S-A) pairs explored by these agents (D_{LG}). Results for Breakout b1, b2, b3 grids, the agent is trained on non-noisy variations of different environments (reported in the headings) and tested in the Low-Noise regime. Rows in the right figure represents agent's actions Left, Right, Stop.
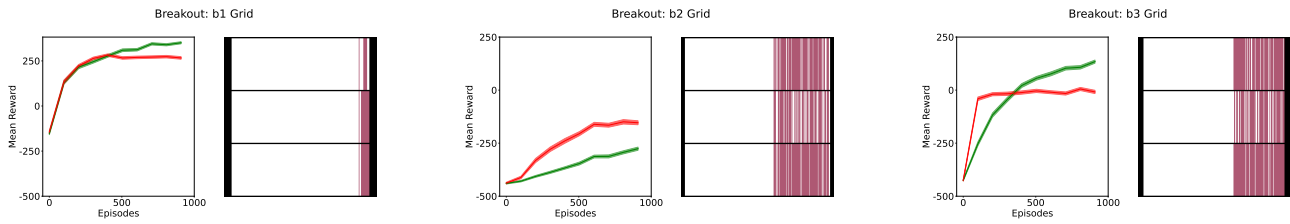
Figure Sup41: *Q-learning Agent with ε-greedy exploration strategy*: The *exploration grid* visualizing the difference in State-Action (S-A) pairs explored by these agents (D_{LG}). Results for Breakout b1, b2, b3 grids, the agent is trained on non-noisy variations of different environments (reported in the headings) and tested in the Low-Noise regime. Rows in the right figure represents agent's actions Left, Right, Stop.
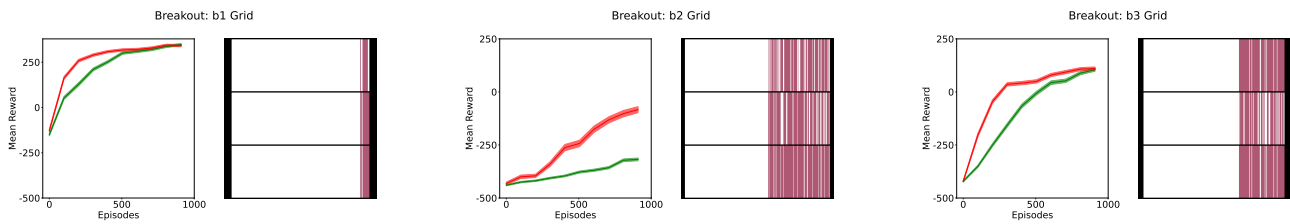

Figure Sup42: *SARSA Agent with Boltzmann exploration strategy*: The *exploration grid* visualizing the difference in State-Action (S-A) pairs explored by these agents (D_{LG}). Results for Breakout b1, b2, b3 grids, the agent is trained on non-noisy variations of different environments (reported in the headings) and tested in the Low-Noise regime. Rows in the right figure represents agent's actions Left, Right, Stop.
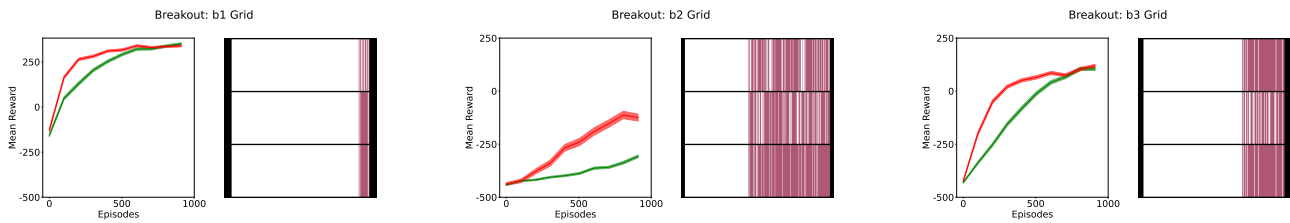

Figure Sup43: *SARSA Agent with ε-greedy exploration strategy*: The *exploration grid* visualizing the difference in State-Action (S-A) pairs explored by these agents (D_{LG}). Results for Breakout b1, b2, b3 grids, the agent is trained on non-noisy variations of different environments (reported in the headings) and tested in the Low-Noise regime. Rows in the right figure represents agent's actions Left, Right, Stop.